This is an open access article published under an ACS AuthorChoice License, which permits copying and redistribution of the article or any adaptations for non-commercial purposes.

Environmental Science & Technology

Critical Review

pubs.acs.org/est

Sulfidation of Iron-Based Materials: A Review of Processes and Implications for Water Treatment and Remediation

Dimin Fan,[†] Ying Lan,[‡] Paul G. Tratnyek,*[,‡] Richard L. Johnson,[‡] Jan Filip,[§] Denis M. O'Carroll,[∥] Ariel Nunez Garcia,[⊥] and Abinash Agrawal[#]

[†]Oak Ridge Institute for Science and Education (ORISE) Fellow, Office of Superfund Remediation and Technology Innovation, U.S. Environmental Protection Agency, 2777 Crystal Drive, Arlington, Virginia 22202, United States

[‡]OHSU-PSU School of Public Health, Oregon Health & Science University, 3181 SW Sam Jackson Park Road, Portland, Oregon 97239, United States

[§]Regional Centre of Advanced Technologies and Materials, Palacký University Olomouc, Šlechtitelů 27, CZ-78371 Olomouc, Czech Republic

[∥]School of Civil and Environmental Engineering, Connected Water Initiative, University of New South Wales, Manly Vale, New South Wales 2093, Australia

[⊥]Department of Civil and Environmental Engineering, Western University, 1151 Richmond St., London, Ontario Canada

[#]Department of Earth and Environmental Sciences, Wright State University, Wright State University, 3640 Colonel Glenn Highway, Dayton, Ohio 45435, United States

Supporting Information

ABSTRACT: Iron-based materials used in water treatment and groundwater remediation—especially micro- and nanosized zerovalent iron (nZVI)—can be more effective when modified with lower-valent forms of sulfur (i.e., "sulfidated"). Controlled sulfidation for this purpose (using sulfide, dithionite, etc.) is the main topic of this review, but insights are derived by comparison with related and comparatively well-characterized processes such as corrosion of iron in sulfidic waters and abiotic natural attenuation by iron sulfide minerals. Material characterization shows that varying sulfidation protocols (e.g., concerted or sequential) and key operational variables (e.g., S/Fe ratio and sulfidation duration) result in materials with structures and morphologies ranging from core−shell to multiphase. A meta-analysis of available kinetic data for dechlorination under anoxic conditions, shows that sulfidation usually increases dechlorination rates, and simultaneously hydrogen production is suppressed. Therefore, sulfidation can greatly improve the efficiency of utilization of reducing equivalents for contaminant removal. This benefit is most likely due to inhibited corrosion as a result of sulfidation. Sulfidation may also favor desirable pathways of contaminant removal, such as (i) dechlorination by reductive elimination rather than hydrogenolysis and (ii) sequestration of metals as sulfides that could be resistant to reoxidation. Under oxic conditions, sulfidation is shown to enhance heterogeneous catalytic oxidation of contaminants. These net effects of sulfidation on contaminant removal by iron-based materials may substantially improve their practical utility for water treatment and remediation of contaminated groundwater.

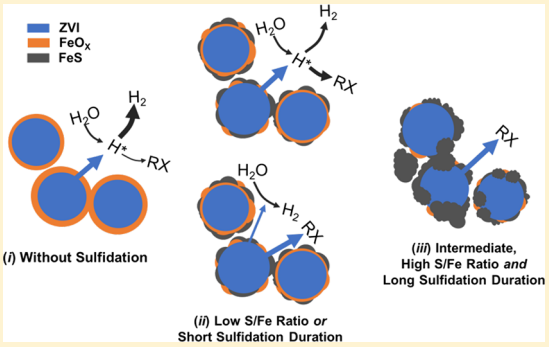

1. INTRODUCTION

Just like "contaminants of emerging concern", most emerging technologies or areas of research are not entirely new, but rather are of renewed interest because of other changes in science, technology, or societal or market factors. Sulfidation exemplifies most aspects of this dynamic, ranging from increased appreciation of previously neglect research to heightened competition among simultaneously initiated studies on this topic. The overall goal of this review is to show-case these dynamics, while at the same time advancing the field through meta-analysis of existing data, cataloging the current state-of-the-art, identifying knowledge gaps, and highlighting opportunities for future research and development.

In general, "sulfidation" (or sulfidization) can refer to any modification or transformation of a metal-based material by exposure to sulfur compounds of various oxidation states, and is most commonly used in geochemistry, corrosion science, and material science for metals with strong affinities for sulfide. There are many such metals of environmental significance (Fe, Cu, Zn, Hg, Ag, Tc, etc.), but iron is by far the most prominent among these. The earliest (electronically indexed) example of

Received: August 14, 2017
Revised: October 13, 2017
Accepted: October 16, 2017
Published: October 16, 2017

Downloaded via 207.241.229.150 on March 21, 2021 at 09:41:54 (UTC).
See https://pubs.acs.org/sharingguidelines for options on how to legitimately share published articles.

this is the work by Rickard et al.[1,2] on the diagenesis of anoxic marine sediments. In that work, they explicitly defined sulfidation as the complex sequence of reactions leading from goethite (α-FeOOH), via metastable iron sulfides, to pyrite (FeS_2). Since then, an extensive literature has developed on Fe and S interactions in biogeochemical processes, mainly involving saturated soils and sediments, including groundwater, but also extending to hyporheic zones, wetlands, and stratified surface waters (e.g., refs 3−6) A mostly separate, but fundamentally related and extensive body of literature concerns sulfidation in the context of oil, gas, and nuclear energy production, which has been motivated by the need to protect iron-based structures, such as pipelines and storage tanks, from both biotic and abiotic sulfur-induced corrosion.[7−11]

In the past few years, interest in sulfidation for environmental applications has increased sharply because of the potential benefits in water treatment and remediation processes—including both reduction and oxidation reactions—resulting from controlled sulfidation of iron, largely nanoscale zerovalent iron (nZVI)[12−23] and recently extended to include microscale zerovalent iron (ZVI)[24,25] and iron oxides (FeO_x)[26] (collectively referred to as "iron-based materials" in this review). However, the majority of these studies introduce the sulfidation concept from the perspective of material synthesis and improvement, often with inadequate appreciation and recognition of the fundamental similarities in chemistry between controlled and natural sulfidation processes. In fact, the emerging interest in controlled sulfidation of iron-based materials for water treatment stems from the convergence of two developments: (i) maturation and diversification of the use of ZVI/iron oxides for water treatment and (ii) the role of iron sulfide minerals in abiotic contaminant transformation processes. Relevant literature in these two areas is scattered across 30 years of research on reactivity of iron and sulfur in biogeochemistry and environmental engineering. Therefore, it is informative to first summarize those areas of research that are—in the context of this review—precursors to recent developments of sulfidated iron-based materials for environmental applications.

2. PRECURSORS TO IRON-BASED MATERIALS SULFIDATION

Starting in the mid 1990s, the prospect of making permeable reactive barriers (PRBs) with ZVI for passive in situ remediation of contaminated groundwater plumes triggered a surge in research into the chemistry of this technology. Most of this work focused on the reduction of organic contaminants coupled to oxidation of the Fe(0) with charge transfer through the partially passivating surface layer dominated by iron oxides.[27] However, several groups recognized that S incorporated in the oxide layer could play a significant role in the overall reactivity of ZVI with contaminants, and reported preliminary results in favor of this hypothesis during the first symposium on contaminant degradation by ZVI at the 1995 ACS National meeting in Anaheim, CA, as well as in several peer-reviewed publications.[28,29] At the time, this work received little attention, even though it soon became evident that sulfide was abundant in ZVI PRBs due to stimulated microbial reduction of sulfate.[30−39] While some other studies used dithionite to treat sediment and surface soil—resulting in sulfidation effects on contaminant degradation—earlier work used dithionite mainly to reduce structural iron, and emphasized the reactivity of reduced iron with contaminants.[40−42] Later, sulfidation of ZVI and its effects on dechlorination was investigated in a series of studies that included extensive characterization of the sulfidated iron phases, by spectroscopy and electrochemistry,[43,44] but even this work received little recognition at the time.

Although ZVI has become the model system used in most studies of abiotic reduction of organic contaminants,[45] the largely independent, parallel literature on contaminant removal by reducing S(−II) species starts earlier and is nearly as extensive. The earliest work in this area was dominated by the dissertations of Barbash,[46] Roberts,[47] and Kriegmen-King,[48,49] which covered the mechanisms and kinetics of abiotic dehalogenation of alkanes and alkenes by aqueous sulfide and pyrite. Subsequent laboratory work focusing on freshly precipitated nanocrystalline mackinawite (FeS) has confirmed repeatedly that the high surface area FeS is reactive with halogenated organic compounds, such as carbon tetrachloride (CT), trichloroethene (TCE), tetrachloroethylene (PCE), and ethylene dibromide (EDB).[50−62] Similarly designed laboratory studies have found that FeS can also be effective for sequestration of various metals, metalloids, and oxyanions, which occurs through a combination of reduction, adsorption and coprecipitation processes.[63−72] These processes certainly apply to ZVI PRBs where sulfate reduction is often significant, but they also are relevant in scenarios where FeS forms under natural conditions, such as hyporheic zones[6] and the rhizosphere in wetlands.[73] The full scope of potential applications of iron sulfides to groundwater remediation—including organics, metals, and radionuclides—was recently reviewed, with emphasis on the applications of FeS nanoparticles for optimal remedial performance.[74]

The favorable effects of Fe/S combinations on contaminant degradation/sequestration identified from laboratory studies have recently been utilized in commercial technologies for in situ remediation of contaminated groundwater. One example of this is the process termed "in situ biogeochemical transformation" (ISBGT),[75−77] which involves creating fresh, high surface area biogenic iron sulfides that react directly with chlorinated solvents. Another commercial application is a microscale ZVI (mZVI) product that contains a slow release sulfate source, which is designed primarily for in situ sequestration of metals. Upon injection of this product, the ZVI initially creates strongly reducing conditions, and microbial sulfate reduction is stimulated in the longer-term. This causes in situ sulfidation of ZVI, which favors precipitation of stable low solubility metal sulfide phases.[78,79]

The prior work on contaminant degradation or sequestration with ZVI and FeS that is summarized above provides the foundation for recent work on contaminant transformations by sulfidated iron-based materials. In early work, sulfidation was considered only as an in situ and/or natural biogeochemical process; whereas interest in sulfidation is now also focused on formulating engineered materials that are composed of multiple phases—especially those based on nZVI—with properties that are optimized for environmental applications. To provide a rational basis for this process of material development, it is necessary to develop a fundamental understanding of the various sulfidation methods and their mechanisms.

3. FUNDAMENTALS OF SULFIDATION

3.1. Methods. Sulfidation has been performed using a variety of sulfidation agents, iron-based materials, and sulfidation processes. The combinations that have been (or

DOI: 10.1021/acs.est.7b04177
Environ. Sci. Technol. 2017, 51, 13070−13085

are soon to be) published are summarized in Table 1, arranged in order of decreasing average valence state of S in the sulfidation agent. Another important organizational theme in Table 1 is the sulfidation process used for sulfidation, which includes aqueous-solid, aqueous−aqueous, solid−solid, and gas−solid. The former two encompass the majority of the sulfidation studies conducted so far and thus will be the main focus of this review. The latter two methods represent recent and ongoing developments, which are included for the sake of completeness.

Table 1. Methods of Sulfidating Iron-Based Materials for (Ground)Water Treatment

sulfidation agent (S valence)[a]	material sulfidated	sulfidation conditions	references[b]
sulfate SO_4^{2-} (+VI)	granular ZVI	aqueous-solid (microbial)	34
	FeO_x		75
sulfur dioxide SO_2 (+IV)	nZVI	gas−solid	80
dithionite $S_2O_4^{2-}$ (+III)	nZVI	aqueous−aqueous	14−16, 19−21, 81−85
		aqueous-solid	86, 87
thiosulfate $S_2O_3^{2-}$ (+II)[c]	nZVI	aqueous-solid and aqueous−aqueous	18
	FeO_x	aqueous−aqueous	22, 26, 88
elemental sulfur S^0 (0)	mZVI	solid−solid	25
sulfide, bisulfide, and polysulfides S^{2-} (−II)	nZVI	aqueous-solid	12, 13, 17, 89
	mZVI		24, 43
	FeO_x		90
thioacetamide $H_3CC(=S)NH_2$ (−II)	nZVI	aqueous-solid	91

[a]Average valence of sulfur in parentheses. [b]Precursory work, only representative references are included. [c]Average sulfur oxidation state does not represent the oxidation state of individual sulfur atoms in thiosulfate.

Aqueous-solid phase sulfidation processes involve reactions between dissolved sulfur species and solid iron materials, like ZVI. Commonly used aqueous sulfur compounds include sulfide (either biogenic or abiotic),[12,13,17,23,34,75] dithionite,[86,87] and thiosulfate.[18] This process has been described as "post-synthesis",[18] and the resulting material is referred to as S-(n)ZVI hereafter. In contrast, aqueous−aqueous sulfidation processes start with soluble sulfur and iron species, in the presence of a strong reducing agent (e.g., $NaBH_4$) if Fe(0) is desired. Both dissolved Fe(II) and newly formed Fe(0) may react concurrently with sulfur to form FeS. This process has been described as "one-pot synthesis"[14] or "pre-synthesis sulfidation",[18] and the resulting material is referred to as Fe/FeS hereafter. Most of the published studies that fall into this group used dithionite as the sulfidation agent. The solution chemistry of this process is highly complex due to multiple reaction intermediates from dithionite oxidation; however, due to the ease of material preparation, this method has been frequently selected. In the absence of a strongly reducing agent and under high pH, sulfidated iron oxides are synthesized.[26,88] The new and novel method of sulfidation by ball-milling ZVI and S(0) is a "two-step" process, but could form relatively uniform materials much like an aqueous−aqueous method, depending on the degree of mechanochemical mixing.[25]

3.2. Mechanisms. Most of what is known about sulfidation mechanisms applies to aqueous-solid sulfidation methods because of its analogy to sulfur induced corrosion, which has been extensively studied in the literature on corrosion of ferrous-metals in sulfidic environments.[8,9,11] Regardless of the sources of sulfur or iron, the reaction between the two is essentially a redox process at the aqueous-solid interface, governed by their thermodynamic equilibrium (Figure 1). Taking sulfide, the most common sulfur source, as an example, it serves as a reductant during sulfidation of Fe(III) oxides (e.g., goethite) by first reducing Fe(III) oxides to Fe(II) via interfacial electron transfer.[4,92] Sorbed sulfide is oxidized to form S(0). If excess aqueous sulfide is available, it reacts with the produced Fe(II) to form FeS,[2] and FeS may continue to

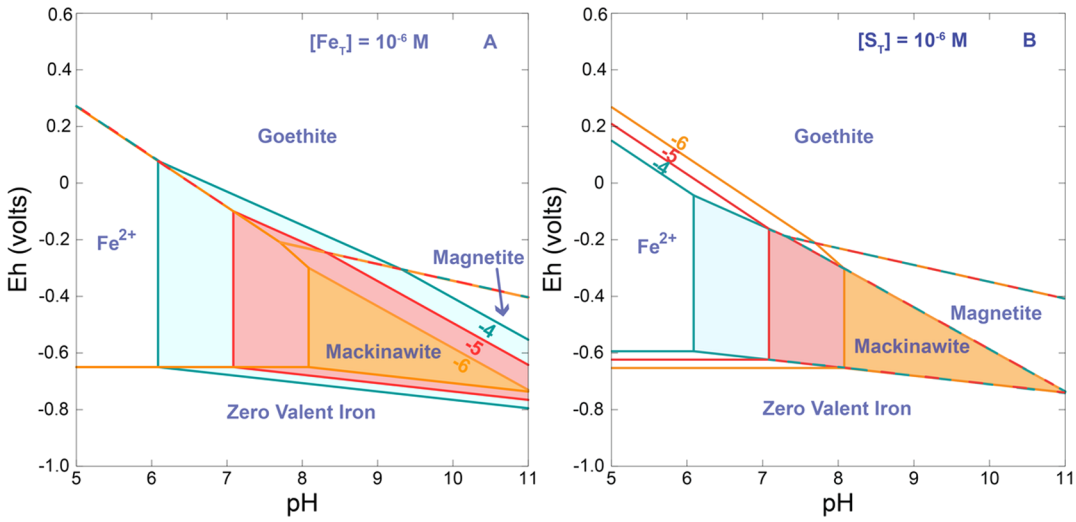

Figure 1. Eh-pH diagram for the Fe−S−H_2O system at 25 °C. Hematite and pyrite are suppressed. Figures were drawn with fixed-concentration species (A: $[S_T] = 10^{-6}$ M, B: $[Fe_T] = 10^{-6}$ M), and contours representing total ions (A: $[Fe_T]$, B: $[S_T]$) were showed in different colors: yellow = 10^{-6} M, red = 10^{-5} M, and blue = 10^{-4} M.

DOI: 10.1021/acs.est.7b04177
Environ. Sci. Technol. 2017, 51, 13070−13085

transform to greigite (Fe_3S_4) and/or pyrite (FeS_2).[93] As for sulfidation of ZVI, the process resembles sulfur-induced corrosion under alkaline conditions,[44] which proceeds via two steps.[44,94−96] The initial step involves rapid adsorption of HS^- onto the Fe(0) surface, replacing previously adsorbed OH^- (eq 1), which then forms a thin layer of FeS on the surface of Fe(0) (eq 2 and 3).

$$Fe - OH^-_{Ads} + HS^- \leftrightarrow Fe - HS^-_{Ads} + OH^- \quad (1)$$

$$Fe - HS^-_{Ads} \leftrightarrow Fe - HS^+_{Ads} + 2e^- \quad (2)$$

$$Fe - HS^+_{Ads} \rightarrow Fe(II) - S_{1-x} + xHS^- + (1 - x)H^+ \quad (3)$$

The enhanced localized acidity (eq 3) can induce localized corrosion of Fe(0), which produces dissolved Fe(II) that then reacts with HS^- to form additional FeS. It has been suggested that the morphological characteristics and protectiveness of the FeS film resulting from these two processes of FeS formation are very different.[94,95] Depending on the sulfidation conditions and duration, the FeS resulting from aqueous precipitation can be either highly corrosive or protective.[95−97] The implication of these dynamics to contaminant transformation by sulfidated iron-based material will be discussed in more detail later (Section 5 and 6).

Compared to sulfide, the mechanism of sulfidation by dithionite is more complicated due to its complex aqueous chemistry and possibly additional interactions between Fe(0) and dithionite or its sulfur intermediates. It is well documented that dithionite at low pH mainly undergoes disproportionation to form thiosulfate (eq 4) and sulfite, whereas it is relatively stable at high pH and slowly decomposes to sulfite and sulfide (eq 5). Either scenario could be relevant depending on whether dithionite is used in aqueous−aqueous or aqueous-solid sulfidation. The former scenario is more relevant during aqueous−aqueous sulfidation as the initial solution pH is acidic and gradually rises to alkaline as reaction proceeds, which may result in different sulfur species at different stages of particle formation. For aqueous-solid sulfidation, dithionite is added to the nZVI suspension that is already alkaline after synthesis (due to synthesis reaction), where Fe(0) may accelerate the decomposition reaction of dithionite by precipitating aqueous sulfide to form FeS. Given the difficulty in tracking and quantifying various sulfur containing intermediates, explanations of the mechanism of sulfidation by dithionite remain speculative and the reaction stoichiometry is unclear.

$$2S_2O_4^{2-} + H_2O \rightarrow S_2O_3^{2-} + 2HSO_3^- \quad (4)$$

$$3S_2O_4^{2-} + 6OH^- \rightarrow 5SO_3^{2-} + S^{2-} + 3H_2O \quad (5)$$

Thiosulfate ($S_2O_3^{2-}$), a strong corrosion promotor under acidic conditions,[8] is relatively stable at high pH, which is more relevant to the aqueous-solid sulfidation scenario. However, in the presence of Fe(0), thiosulfate is readily reduced to HS^-, which is more stable according to the thermodynamic speciation modeling.[8] Experimental evidence for this was presented in an early study on corrosion of Fe-17Cr alloy by thiosulfate at (circum)neutral pHs.[98] In that study, it was found that thiosulfate was only corrosive when reduced to sulfide, and that the reduction reaction only occurred on the bare surface of the metal, not on the passive film, suggesting that the metal might be the source of the reductant. If these results apply under environmental conditions, Fe(0) should reduce thiosulfate to sulfide before sulfidation takes place. Similar redox reactions may also occur for gas−solid sulfidation (e.g., between preformed Fe(0) and sulfur dioxide at elevated temperature[80]) and solid−solid sulfidation (e.g., between Fe(0) and elemental sulfur (S(0)) by mechanochemical processes such as ball milling[25]).

4. CHARACTERIZATIONS OF SULFIDATED IRON-BASED MATERIALS

Compared to the material characterizations conducted in the precursory work on sulfidation of iron-based materials, which were mostly limited to identifying FeS minerals in ZVI-based PRBs,[30,33,34] more recent studies on sulfidation of iron-based materials (mostly nZVI) have placed greater emphasis on qualitative and quantitative characterizations of the properties of sulfidated materials. These materials were prepared under a wide range of conditions—including processes, operational and experimental variables—some of which are summarized in Table 1. A holistic examination of these characterization results is presented below to identify common features and differences to determine the major factors that control properties of sulfidated materials. The following section focuses on the two most relevant aspects of these characterizations, featuring nZVI as an example: mineralogy and morphology. Other characterization methods have been used—such as electrochemistry[15,81,99]—but are not included.

4.1. Bulk Mineralogy and Surface Composition. Bulk characterizations of mineralogy and composition of sulfidated nZVI mainly concern two aspects: the characteristics of FeS and the amount of Fe(0) remaining. The FeS phases formed in sulfidation studies are mainly amorphous or nanocrystalline mackinawite, according to X-ray diffraction (XRD) data.[12,20,83] It is usually the first metastable iron sulfide phase formed in sulfidic environments.[2] Further transformation to crystalline mackinawite and more stable pyrite requires relatively long reaction times, like those often used in corrosion studies.[90,97,100] Given the limited utility of XRD in characterizing amorphous phases and phases present at low content (e.g., as a thin surface layer), X-ray photoelectron spectroscopy (XPS) is usually used to probe the changes of surface species and chemical states that take place on the surface of sulfidated materials. Comparing the XPS spectra collected in various studies shows consistency in the S 2p XPS spectra of sulfidated nZVI, generally indicating the presence of monosulfide (S^{2-}), disulfide (S_2^{2-}), and other polysulfide species, regardless of sulfur sources or processes.[12,14,17,18,20,81,86] In contrast, their Fe 2p spectra counterparts can be clearly divided into two groups (Supporting Information (SI) Figure S1). One group shows a much lower FeS peak than the other, suggesting lower surface abundance of FeS.[12,14,82,86] It was found that the spectra with weak FeS signal mainly came from studies that either used aqueous−aqueous sulfidation or used aqueous-solid sulfidation but with short sulfidation duration; whereas a larger FeS peak was observed only in studies that utilized high S/Fe ratio and long sulfidation duration. This is expected because aqueous−aqueous sulfidation results in simultaneous precipitation of FeS and Fe(0) and hence more uniform distribution of S. For aqueous-solid sulfidation, longer sulfidation duration may accumulate more FeS on the surface, leading to a larger peak from FeS and shielding of the spectral band of Fe(0).

The remaining Fe(0) content after sulfidation is the other important factor, as Fe(0) accounts for the majority of the reducing capacity of nZVI. Although it is expected that the

DOI: 10.1021/acs.est.7b04177
Environ. Sci. Technol. 2017, 51, 13070−13085

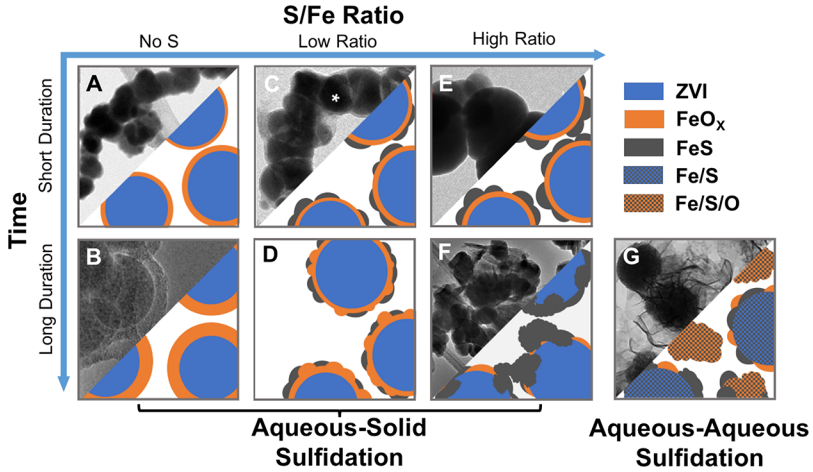

Figure 2. Conceptual model of sulfidated nZVI prepared using aqueous-solid sulfidation (C−F) and aqueous−aqueous sulfidation (G), with corresponding TEM images. (A) nZVI core with thin FeO_x shell (TEM:[105] freshly prepared nZVI) (B) nZVI core with thick FeO_x shell (TEM:[12] nZVI in synthetic groundwater buffered at pH 7.9, t = 24 h); (C) S-nZVI with low S/Fe ratio and short sulfidation duration (TEM:[17] S/Fe = 0.04, t = 10 min); (D) S-nZVI with low S/Fe ratio and long sulfidation duration; (E) S-nZVI with high S/Fe ratio and short sulfidation duration (TEM:[17] S/Fe = 0.08, t = 10 min); (F) S-nZVI with high S/Fe ratio and long sulfidation duration (TEM:[12] S/Fe = 0.112, t = 24 h) (G) Fe/FeS, formed via aqueous−aqueous synthesis (TEM:[20] S/Fe = 0.28).

remaining Fe(0) would decrease with increasing S/Fe ratio, several studies have shown that the degree of sulfidation plateaued above a given S/Fe ratio. For example, for laboratory prepared nZVI, Mössbauer spectra of S-nZVI showed that a S/Fe ratio of 1.12 after 24 h sulfidation resulted in only 10% of Fe(0) transforming to FeS, which is the same as the S/Fe ratio of 0.112, likely due to inhibited corrosion at high S/Fe ratio.[12] A similar observation was also reported for nZVI synthesized on carboxylmethylcelluose (CMC-nZVI)—using hydrogen measurements after acidification—that the low and high S/Fe ratio (0.33 and 1) recovered similar amounts of Fe(0) when sulfide was used for sulfidation.[13] However, when dithionite was used for sulfidation, substantially more Fe(0) is converted to FeS at both low and high S/Fe ratios, suggesting that dithionite is a more aggressive sulfidation reagent than sulfide.[13]

4.2. Microscopic Structure and Morphology. Microscopic characterizations from existing sulfidation studies further support the bulk characterization results by showing that the type of sulfidation process and two main operational variables (S/Fe ratio and sulfidation duration) play major roles in affecting the structure and morphology of sulfidated materials. This is illustrated in Figure 2, which shows conceptual models of S-nZVI prepared using aqueous-solid methods (Figures 2C, 2E and 2F) and Fe/FeS prepared using aqueous−aqueous methods (Figure 2G), arranged as a function of sulfidation duration (y-axis) and S/Fe ratio (x-axis). Each conceptual cartoon describes the key features of the material, and is accompanied by a published transmission electron microscopy (TEM) image, when available, of sulfidated material prepared under similar conditions. To highlight the effects of operational variables while minimizing other variables, only nZVI synthesized by borohydride reduction is included among the TEMs shown.

For unmodified nZVI, it has been shown repeatedly that exposure in water results in shrinking of the Fe(0) core and increasing thickness of the oxide shell,[101−104] which can be seen in Figures 2A and 2B. When sulfide was introduced to react with the nZVI (i.e., aqueous−solid sulfidation), the resulting materials appear to fall into two groups. The short sulfidation duration appears to preserve the chain-like and the core−shell structure of the original nZVI (Figures 2C and E). Comparison between Figures 2C and E shows no significant morphological change between S/Fe ratios of 0.04 and 0.08. However, residual aqueous sulfur measurements at the end of sulfidation did show increasing sulfur sequestration by nZVI at higher S/Fe ratios, likely suggesting increasing FeS coverage or thickness.[17] With increasing sulfidation duration, sulfidation is expected to continue, resulting in precipitation of secondary FeS, which has a distinct flake-like structure and is associated with the nZVI-like structure (Figure 2F: S/Fe = 0.112 and t = 24 h).

The morphological transition over time is similar to the process described during sulfur induced corrosion.[44,95,100] In this process, a thin layer of FeS forms initially upon brief exposure of steel to sulfide by chemisorption.[44,95] A secondary FeS layer may then form, upon extended exposure in a sulfidic environment. A similar process has also been described for the morphological changes of silver nanoparticles (AgNP) during sulfidation with increasing S/Ag ratio.[106] The formation of a thin sulfur layer on S-nZVI was also observed in our preliminary characterizations of oxide-free nZVI (prepared by thermal reduction) treated with 1% sulfide for 5 min (SI Figure S2). However, elemental mapping indicates that the sulfur layer was underneath an oxygen-rich layer. This is inconsistent with the XPS results of S-nZVI (synthesized by borohydride reduction), which show sulfur abundance decreased with increasing depth from the surface.[17] The reason for this discrepancy is unclear, but it could arise because the oxide-free nZVI undergoes simultaneous sulfidation and dissolution/reprecipitation.

For Fe/FeS formed via aqueous−aqueous methods, microscopic characterization revealed that the resulting material contains both spherical and flake-like structures (Figure 2G), which appear to be analogous to the original Fe(0) and the secondary FeS, respectively, shown in Figure 2F (S/Fe = 0.112, t = 24 h). However, energy dispersive X-ray spectroscopy (EDX) showed that the core actually has slightly higher S content than the flakes,[20] which cannot be explained by the Fe(0)-FeS core−shell model used to describe materials made by the aqueous-solid method. The authors proposed an alternative hypothesis that as sulfidation proceeds, it results in

DOI: 10.1021/acs.est.7b04177
Environ. Sci. Technol. 2017, 51, 13070−13085

a core that is mainly composed of Fe(0) and S(0), and flakes that are a mixture of FeS and iron (hydr)oxides.[20] The distinctly different patterns of S distribution observed with the different sulfidation processes agrees with the reported XPS Fe 2p spectra (SI Figure S1) showing that aqueous−aqueous sulfidation results in lower abundance of surface FeS despite comparable or even a higher S/Fe ratio than aqueous-solid sulfidation. Surface layers are also less prominent in materials sulfidated by mechanochemical mixing (i.e., ball milling).[25] Together, these results indicate that different sulfidation processes result in particles with distinct properties, which may have important implications to their reactivity with contaminants.

5. EFFECTS OF SULFIDATION ON CONTAMINANT TRANSFORMATION

5.1. Metals and Metalloids. Mechanisms, Products, and Kinetics. The currently available studies on removal of metals and metalloids by sulfidated iron-based materials[12,20,83,107,108] suggest that sulfidation can have profound effects on mechanisms, products, and kinetics in these systems. An early and prominent example investigated the sequestration of pertechnetate (TcO_4^-, a Tc(VII) metal oxyanion and long-lived radionuclide of concern) by nZVI with and without sulfidation (using sulfide).[12] In both systems, Tc(VII) was reduced to Tc(IV), but the speciation of the Tc(IV) shifted from TcO_2 to TcS_2 with increasing S/Fe ratio. TcS_2 became the dominant product at S/Fe as low as 0.05, suggesting that the reduction of TcO_4^- by FeS is favorable enough to be the preferred sequestration pathway even in the presence of nZVI. This resulted in increased rates of TcO_4^- removal up to S/Fe = 0.112, but TcO_4^- removal rates decreased at higher S/Fe, which was shown to be due to inhibition by excess aqueous sulfide.[12] A similar peak in removal rates at intermediate S/Fe was observed for the metal oxyanion chromate (CrO_4^-), also at S/Fe ≈ 0.11, although Cr(III) oxyhydroxides were the only products across the whole range of S/Fe.[23]

Among metal cations of environmental concern (Cu, Pb, Cd, etc.), many interact strongly with S due to the low solubility of their metal sulfide phases,[109] but only cadmium (Cd) has been used to investigate the effect of sulfidation on sequestration of metals by nZVI.[20] Using dithionite as a sulfidation agent, the quantity of Cd removed after 2 h of contact with Fe/FeS was found to decrease and then increase with S/Fe, resulting in a minimum at S/Fe ≈ 0.07. This trend, while opposite to what has been seen with the removal kinetics of metal oxyanions (e.g., Tc), may be due to similar changes in the sequestration mechanism. In this case, it was proposed Cd sequestration at low S/Fe is dominated by adsorption and surface complexation on nZVI, whereas displacement of Fe(II) in FeS becomes dominant at high S/Fe ratios, resulting in the formation of (Fe, Cd)S phases, which were detected by XPS.[20]

Although the metals discussed above only represent a small subset of metals and metalloids of environmental concern, the reported effects of sulfidation should also apply to other metals and metalloids because of similar underlying mechanisms that control their removal by iron-based materials. For example, it is well established that the removal mechanisms of metals/metalloids by unsulfidated nZVI are primarily controlled by their reduction potentials.[103,110] Metals/metalloids with significantly higher standard reduction potentials than Fe(0), such as Cu(II), Ag(I), and SeO_4^{2-}, are removed predominantly by reductive immobilization,[111,112] whereas those with similar or lower standard reduction potential than Fe(0) (e.g., Zn(II)), are removed primarily via nonredox based adsorption or precipitation.[103] In contrast, for FeS, the solubility of the metal sulfide phases is shown to govern the removal mechanisms.[109] Thus, it is expected that sulfidation of iron-based material may shift the removal of the metals and metalloids (especially those have strong affinity to sulfide, such as Hg) from a redox potential controlled process to a solubility controlled process (Figure 3). For metalloids that have multiple oxidation states,

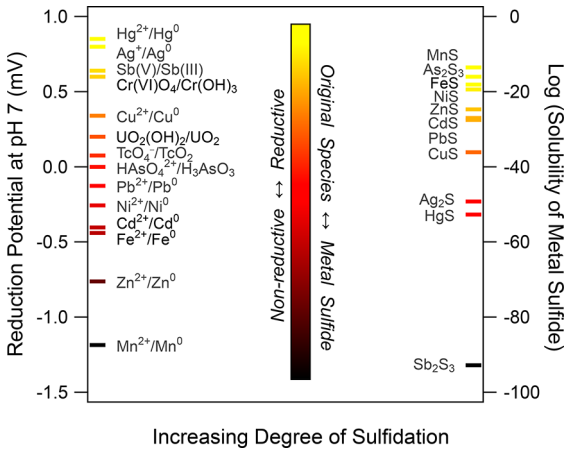

Figure 3. Sequestration mechanisms for representative metal and metalloid contaminants by ZVI and FeS, with the expected shift of sequestration mechanism upon sulfidation (Left axis: the redox couples are positioned based on their formal reduction potential at pH 7; Right axis: the metal sulfide phases are positioned based on their solubility constant; The color gradient represents gradual shift from one sequestration mechanism to another).

such as arsenic or selenium, more complexity could arise as different experimental variables (e.g., pH, contaminant concentrations, redox condition, iron types or sulfur levels) could all result in a diverse range of sequestration pathways and products for both sulfidated and unsulfidated materials, as shown by multiple studies.[68,113,114] This diversity will become a challenge as new studies on contaminant metal sequestration by sulfidated ZVI become available, but general principles (e.g., structure−activity relationships for metals sequestration, such as in Kim et al.[15]) should eventually emerge.

Stability of Sequestration Products. Sequestration of metals and metalloids by sulfidated iron-based materials is favorable under anoxic, reducing conditions. However, subsurface redox conditions can fluctuate between reducing and oxidizing as a result of natural (e.g., flooding, surface water intrusion, seasonal water table fluctuations) or anthropogenic (e.g., dredging) events, and these changes may affect the long-term stability of sequestrated metals and metalloids.[107,115,116] Under nonsulfidic conditions, oxidative remobilization of metals—e.g., U and Tc—has been demonstrated by common natural oxidants, including dissolved oxygen, manganese dioxide (MnO_2), and nitrate, which oxidize these metals, either abiotically or biotically.[117−123]

Among the metals for which sequestration by sulfidated ZVI is well characterized, reoxidation of the sequestration products has been studied only for Tc.[107] Starting with the multiphase material formed from TcO_4^- exposed to S-nZVI, it was shown that Tc reoxidation became slower with increasing S/Fe, which is consistent with other evidence that TcS_2 is less susceptible to

DOI: 10.1021/acs.est.7b04177
Environ. Sci. Technol. 2017, 51, 13070−13085

oxidation than TcO_2. It was shown that oxidation of TcS_2 occurs via TcO_2, which may contribute to the slower oxidation rates of the former. It was also found that FeS acts as a redox buffer by scavenging dissolved oxygen, which further inhibits Tc reoxidation. The latter was evidenced by a lag phase, during which no aqueous Tc was measured, followed by a sharp increase in aqueous Tc that was concurrent with the rapid increase of solution oxidation−reduction potential (ORP). Similar observations have been reported for UO_2, Cr(VI), and As(III) in pure FeS systems.[118,121,124,125] For As(III), the resulting As(V) sorbs strongly to the iron oxyhydroxides that form at high pH, thereby prevented remobilization.[125] However, for Cr(VI) reduction by FeS, where Fe−Cr solids were formed, upon exposure to the oxidant, significant dissolved Cr(VI) was released;[121] for UO_2, depletion of FeS also results in complete remobilization of uranium.[118] This range of results suggest that the long-term stability of metals and metalloids sequestered by sulfidated iron-based materials may vary significantly depending on the characteristic interactions between metals/metalloids and iron mineral phases.

5.2. Organic Contaminants. To date, most of the interest in sulfidation of iron-based materials arises from its beneficial effects on the degradation of organic contaminants, where the collective benefits may contribute substantially to overcoming the issues that have limited application of existing iron-based remediation and water treatment technologies.[126] Developments in this area have focused on oxidation or reduction. Reduction is mostly relevant in groundwater treatment under anoxic conditions, where sulfidated (n)ZVI is used as the primary reductant to degrade halogenated compounds (mainly chlorinated aliphatic compounds but recently including a couple of brominated flame retardants as well as one antibiotic).[13−18,81,82,127] Oxidation mostly concerns surface water and wastewater treatment under oxic conditions, where sulfidated iron oxides or (n)ZVI serve as catalysts in oxidation process for treating a variety of organic contaminants.[22,26,85,88,89,128] This section discusses both processes, but with the main focus on reduction as sulfidated iron-based materials are directly involved in contaminant degradation. In addition, literature on reduction is more abundant, allowing a more in-depth analysis.

Reduction Mechanisms. The products, pathways, and mechanisms of abiotic dechlorination of chlorinated aliphatic compounds have been characterized extensively using model systems based on (n)ZVI and various iron oxides and sulfides.[129,130] In all of these systems, reductive β-elimination pathways generally predominate over hydrogenolysis pathways for chlorinated ethenes like TCE,[130−133] so a major change in dechlorination pathways is not expected upon sulfidation of (n)ZVI. This is consistent with results reported to date on TCE reduction by sulfidated nZVI, which identified mainly the β-elimination products, such as acetylene, ethene, and ethane.[18,25] Abiotic dechlorination of CT generally occurs mainly by hydrogenolysis for both ZVI[134] and FeS,[130] and this is expected to apply to sulfidated iron-based reductants as well. Both reductive elimination and hydrogenolysis have also been reported for abiotic debromination, and a series of studies on brominated flame retardants has shown that the branching between these pathways is not greatly affected by sulfidation, although it is strongly influenced by the degree of halogenation of the specific contaminant.[81,82]

From the reductant perspective, there has been a great deal of work on identification of the specific reducing species (Fe(0) or Fe(II) surface species, surface bound atomic hydrogen, S(-II) species, etc.) that are responsible for abiotic dehalogenation by ZVI, iron oxides, and sulfides.[132,135−137] This background should also apply to sulfidated iron-based reductants, but some clear differences are expected depending on material composition. For example, there is evidence for both H-transfer and electron-transfer from (n)ZVI,[136,138] whereas FeS can donate electrons but does not produce atomic H. For the (n)ZVI system, there is evidence that the relative significance of contaminant reduction by direct electron transfer versus the indirect route via activated hydrogen varies with a variety of factors, especially contaminant type. In particular, early studies with (n)ZVI concluded that the primary TCE degradation mechanism is via atomic hydrogen, whereas degradation of CT proceeds via electron transfer.[137−140] For FeS (in the absence of (n)ZVI), dechlorination must be by electron transfer, although it is not entirely clear if the donor sites are Fe or S.[51,62,81] For sulfidated (n)ZVI, the relative contribution of atomic hydrogen versus Fe (or S) electron-donor surface sites to contaminant reduction is an active area of research and debate, as elaborated below. New work on this topic is expected, in part because a better understanding of the beneficial effects of sulfidation on contaminant degradation will aid in its optimization for practical applications in remediation.

Reduction Kinetics. Recent work on sulfidation, like the many studies using various ways to enhance the utility of ZVI for remediation (bimetallic amendments, nanosized particles, oxygenation, etc.), have emphasized increased rates of contaminant removal as a major benefit.[14,17,18,25] However, most of these conclusions are based on comparisons between control and sulfidation effects under a narrow range of conditions, so the generality of such results merits further consideration. To address this, we compiled most of the kinetic data that are currently available for reduction of chlorinated organics by iron-based reductants, and subjected them to the meta-analysis shown in Figure 4. By far, the majority of data available are for CT and TCE, which are summarized in the format of surface area normalized rate constant (k_{SA}) vs mass normalized rate constant (k_M) in Figures 4A and 4B, respectively. For both contaminants, the available data obtained with sulfidated reductants are shown with open markers and solid circles are used for nonsulfidated iron-based materials (including nZVI, microscale ZVI of various purities, FeS, and iron oxides). For CT (Figure 4A), the data for sulfidated materials form clusters roughly coincident with data obtained with nonsulfidated forms of the same material, suggesting that sulfidation does not generally increase rates of CT degradation. In contrast, the TCE kinetic data (Figure 4B) show at least 1 order of magnitude increase in k_M and/or k_{SA} for sulfidated materials compared with their nonsulfidated analogs, and there is sufficient data to conclude that this enhancement probably applies over most conditions. To further illustrate and extend this analysis, Figure 4C shows the ratio of k_M for sulfidated versus nonsulfidated nZVI for CT and TCE and the other contaminants for which a limited amount of kinetic data are available. In this representation, the diagonal contours represent the enhancement factor, R (defined in ref 24). Figure 4C clearly shows that R for TCE is significantly greater than 1 (∼50), CT and HBCD are roughly 1 (i.e., no enhancement), and the data on other contaminants are too

DOI: 10.1021/acs.est.7b04177
Environ. Sci. Technol. 2017, 51, 13070−13085

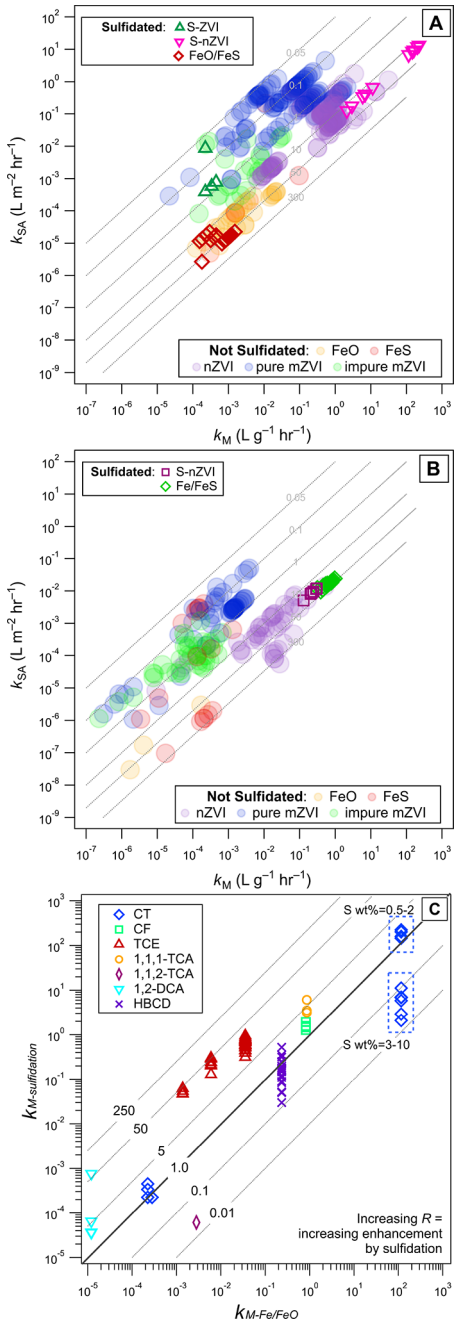

Figure 4. Comparison of rate constants for contaminant reduction by reducing materials with and without sulfidation: (A) k_{SA} vs k_M plot for CT (331 k's from 21 refs[43,53,134,135,138,143−158]); (B) k_{SA} vs k_M plot for TCE (189 k's from 24 refs[14−17,52,54,56,60,132,133,148,152,159−170]); (C) k_M with sulfidation vs k_M without (95 k's from 8 refs[14,16−18,43,82,86,143]). The diagonal contours in (A) and (B) represent specific surface areas used to calculate k_{SA} and the contours in (C) represent the relative effect of treatment (R). Elaboration on the format of these graphs can be found where they were first used: (A,B)[155] and (C).[24] All of the data plotted for (C) are given in SI Table S1.

sparse to generalize, except that the overall range in R is roughly from 50 to 0.1, depending on the S/Fe ratio (which is discussed in detail later).

The contrasting effect of sulfidation on reduction rates of TCE and CT may be a reflection of differences in dechlorinating species for these two contaminants. Specifically, it has been hypothesized that surface sulfur poisons the recombination of atomic hydrogen to form H_2, thereby leaving more atomic hydrogen at the surface for TCE degradation.[18] This hypothesis is supported by data showing (i) no enhancement of CT reduction (which occurs predominantly by electron transfer) at S/Fe of 0.05, (ii) a similar enhancement of TCE degradation rates by adding another known poison for atomic hydrogen recombination (i.e., arsenic[141]), and (iii) the decrease in H_2 formation.[18] However, this hypothesis may be inconsistent with other data, such as the increasing TCE reduction rate by S-nZVI with increasing pH, which has been observed with both S-nZVI[17] and Fe/FeS.[16] This pH dependence is opposite that for H_2 formation by ZVI corrosion (and therefore, presumably, the availability of surface H, which is an intermediate in the formation of H_2). Furthermore, the observed pH dependence of TCE degradation by sulfidated nZVI is consistent with the pH effect observed with pure nanocrystalline FeS,[51] but opposite to the trend with unmodified nZVI.[140] Prior studies on TCE degradation by pure FeS have noted that higher pH increases the negative charge of FeS surface, thereby providing increased driving force for electron transfer.[51,54] These results favor an alternative hypothesis proposed by Rajajayavel et al.,[17] that TCE reduction by S-nZVI occurs predominantly via FeS, which serves as a mediator of electron transfer from Fe(0) to FeS-sorbed contaminants. This also is consistent with the high electron conductivity of FeS,[142] and the inhibited H_2 production from S-nZVI may simply be due to FeS blocking direct access of water to Fe(0) sites (see conceptual model presented below).

The operational variable that seems to have the greatest overall effect on the kinetics of contaminant reduction by sulfidated nZVI is the S/Fe ratio. For all contaminant types, sulfur sources, and sulfidation methods, contaminant reduction rates increase from low to moderate S/Fe ratios and then plateau or decrease at high S/Fe ratios. For most contaminants shown in Figure 4C, this trend is hard to track in the figure due to the closeness of data points, but can be observed by comparing the k_M in SI Table S1. One distinct example is CT (Figure 4C), for which the data suggest a small enhancement at the lowest S/Fe ratios, and inhibition at increased S/Fe ratios (i.e., $R \leq 1$).[143] The consistency of the trend in R with S/Fe ratio suggests that there is a set of controlling factors that is common to all conditions, most likely the formation of FeS and its subsequent effects on corrosion of Fe(0). Nevertheless, the range of R among different contaminants may indicate different sensitivities to various operational variables.

Reduction Pathway Selectivity. While most of the above kinetic studies have focused on enhanced contaminant degradation by nZVI due to sulfidation, they generally have not emphasized or appreciated the fact that the enhanced contaminant degradation may be caused, at least in part, by improved selectivity of nZVI between contaminant degradation and H_2 production. This selectivity is quantified by the ratio of electrons used for contaminant degradation and electrons consumed by natural reductant demand (NRD).[126] The partial inhibition of hydrogen production by sulfidated nZVI noted in two kinetics studies implies that more Fe(0) could become available for contaminant degradation.[17,18,25] A comprehensive evaluation of the effects of sulfidation on selectivity showed complete inhibition of H_2 production achieved for CMC-nZVI sulfidated for 24 h at high S/Fe ratios.[13] In contrast, nonsulfidated CMC-nZVI was completely oxidized by H_2O in <2 days, which is consistent with other laboratory data showing that selectivity of nZVI for contaminant degradation is poor

DOI: 10.1021/acs.est.7b04177
Environ. Sci. Technol. 2017, 51, 13070−13085

because most Fe(0) is consumed by water to form H_2.[126,132,171−173]

More importantly, H_2 measured after acidification of sulfidated nZVI indicated that the majority of the initial Fe(0) input was recovered, suggesting preservation of Fe(0). As both high S/Fe ratio and long sulfidation duration were used, it is reasonable to expect, based on Figure 2F, that secondary FeS precipitates could form, which caused complete inhibition of corrosion. This is consistent with the corrosion literature, suggesting that under conditions similar to aqueous-solid sulfidation (e.g., above neutral pH and excess aqueous sulfide), the effects of secondary FeS layer on corrosion is inhibitory instead of promoting.[44,94,95] These findings also indicate that the partial inhibition of hydrogen production observed in studies applying short sulfidation duration is more likely due to incomplete inhibition of corrosion, given the absence of secondary FeS precipitates with short sulfidation duration (Figure 2C and E).

Improved selectivity results in enhanced persistence of abiotic degradation. This effect may be of even greater practical significance than reactivity enhancement because persistence and longevity are more important than reactivity in coping with in situ treatment of subsurface contamination that is often limited by mass transfer processes (e.g., dissolution or diffusion). Laboratory studies have shown that sulfidated nZVI is a more persistent reductant and even extended aging produced little loss in reactivity with TCE,[13] 1,2-DCA,[86] and tetrabromobisphenol A (TBBPA).[81]

Another potentially significant effect of sulfidation on selectivity involves the competition between abiotic and biotic dechlorination. This has not been included in traditionally defined selectivity (i.e., contaminant vs natural reductant demand) in prior literature, but is discussed here because of its significant and broad field implications for both nZVI and mZVI. A common rationale for ZVI application is that the corrosion of Fe(0) produces H_2 that is beneficial to biological dechlorination. However, this scenario may not always be desirable because the biological process is difficult to control and may produce recalcitrant intermediates such as *cis*-DCE and vinyl chloride. In fact, biological dechlorination (although not due to hydrogen production) has undercut the success of ISBGT at several sites, where abiotic dechlorination was outcompeted, leading to stalled degradation at *cis*-DCE.[174] With sulfidation, limited hydrogen production may selectively inhibit biological processes during ZVI application and preserve reducing capacity for more persistent abiotic degradation.

Reduction Conceptual Model. The above discussion suggests that major benefits of sulfidation of ZVI for degradation of organic contaminants—enhanced reactivity and improved selectivity—are controlled by well-established effects of S on the corrosion of Fe(0). These effects are most strongly influenced by two operational variables: S/Fe ratio and sulfidation duration. Variations in these operational variables affect the growth and evolution of the FeS layer, which become feed-backs that influence further corrosion of the material and degradation of contaminants. To summarize these effects, a conceptual model is shown in Figure 5.

At low S/Fe ratio or short sulfidation duration (Figure 5(ii)), the initial chemical sorption of sulfide ion to the surface results in formation of a thin and dense layer of FeS (SI Figure S2), which is favored at high pH during sulfidation. The layer plays an overall inhibitory role with respect to corrosion, but intraparticle aggregation may cause nonuniform distribution of

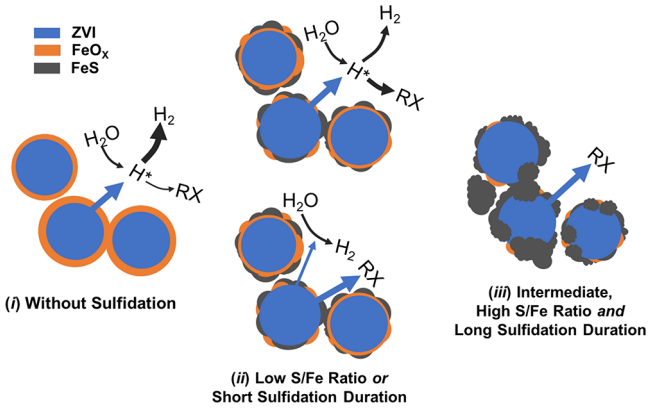

Figure 5. Conceptual model for the effects of aqueous-solid sulfidation of nZVI on degradation kinetics and selectivity of organic contaminants. Three scenarios are included: (i) no sulfidation; (ii) low S/Fe or short sulfidation duration; and (iii) intermediate and high S/Fe ratio and long sulfidation duration. The thick arrows highlight the dominant reactions; RX represents TCE, CT or other alkyl halides.

FeS, leaving less sulfidated surface susceptible to corrosion to produce H_2. The model in Figure 5 includes both atomic hydrogen and electron transfer scenarios. Even though our analysis suggests the latter is a more likely mechanism, existing data is insufficient to exclude the possible role of atomic hydrogen, especially at very low S/Fe ratios. The degradation product distribution at S/Fe = 0.00125 had a similar pattern as unmodified nZVI, which is distinct from treatments at higher S/Fe ratios.[18] Under these conditions, examining degradation kinetics at various pHs may provide additional data to assess the importance of atomic hydrogen. As S/Fe further increases (Figure 5(iii)), surface coverage of the FeS layer becomes more extensive and secondary FeS layers might form, which may completely inhibit corrosion. However, it is worth noting that such a layer may only form when sufficiently long sulfidation duration is given to allow the temporal accumulation and evolution of the surface precipitates, as shown in the corrosion literature.[100,175]

Oxidation. Research on using sulfidated iron-based materials for oxidative degradation of contaminants has evolved in parallel with reduction. Much of it has studied sulfur-doped iron oxides (prepared by aqueous−aqueous sulfidation approach using thiosulfate),[22,26,88,128] but only recently has sulfidated (n)ZVI been shown to catalyze oxidative contaminant degradation processes.[84,89,91] The latter is part of an emerging trend of applying (n)ZVI in aerobic processes for metal/metalloid sequestration and organic oxidation.[176−181] Under aerobic conditions, iron-based materials usually are not directly responsible for contaminant oxidation; instead, they catalyze the formation of highly reactive oxidizing species, such as various reactive oxygen species (especially hydroxyl radical) or sulfate radical. Comparison of the catalytic activity between nonsulfidated and sulfidated materials consistently shows that sulfidation improves the oxidation kinetics of various types of contaminants by a range of oxidants that are commonly used in advanced oxidation processes (AOP), including hydrogen peroxide,[26,88] persulfate,[22,84] or simply under aerobic conditions,[85,91] where dissolved oxygen is activated to form H_2O_2. The effect of sulfidation on these oxidative processes has been attributed to accelerated electron transfer between oxidant and iron species by sulfidation at the material surface, thus enhancing activation of oxidants. This is supported by electron

DOI: 10.1021/acs.est.7b04177
Environ. Sci. Technol. 2017, 51, 13070−13085

paramagnetic resonance (EPR) performed on Fe/FeS prepared using dithionite, showing increasing abundance of hydroxyl and superoxide radicals with increasing S/Fe.[85] However, degradation rates were slower at higher S/Fe, again in common with the bimodal trend observed in reduction. As with reductive processes, this pattern was attributed to mineralogical and morphological changes in the material with increasing S/Fe, such as increasing formation of iron oxides.

6. IMPLICATIONS FOR GROUNDWATER REMEDIATION AND WATER TREATMENT

The use of ZVI and other reducing iron-based materials in environmental engineering applications has undergone significant growth in the past decade, including (i) in situ applications for the remediation of contaminated groundwater, where conditions are relatively anoxic and contaminant removal is predominantly due to reductive processes, and (ii) ex situ applications for treatment of drinking-, waste-, and industrial process waters, where oxic conditions lead to oxidative processes for contaminant removal. Some of this has been driven, and enabled, by efforts to expand the scope of application of ZVI using nanoscale particles, with sulfidation now quickly becoming a similarly important theme. The relationship between these trends is summarized in Figure 6, with the intersections involving the sulfidation sphere corresponding to the aspects that are most relevant to the scope of this review.

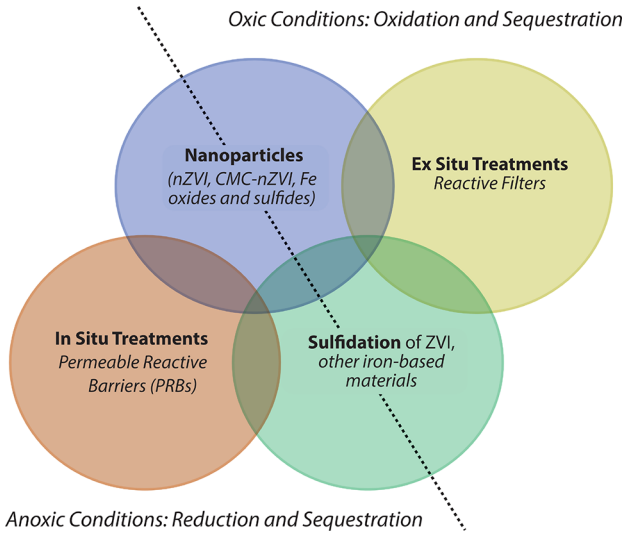

Figure 6. Relationship between four major aspects of water treatment using ZVI and related iron-based materials. Those mainly applicable to suboxic conditions—especially groundwater—are grouped in the lower-left. Those that are mainly applicable to oxic conditions—such as industrial wastewater—are shown in the upper right. The diagonal line separates applications that are primarily suboxic from oxic. The circles are all the same size for convenience.

Sulfidated iron-based materials have been used in field-scale groundwater remediation applications as far back as the late 1990s. Most of these were ZVI-based PRBs constructed to treat heavy metal contamination in high-sulfate groundwater by sequestration of the contaminants as low solubility metal sulfides.[36,37,182,183] The sulfide at these sites was biogenic from natural sulfate reduction, and relatively little attention was given to how this sulfide altered the composition and reactivity of the ZVI. More recently, there has been field-scale testing of ways to stimulate in situ formation of FeS without involvement of Fe(0). Most of these—now referred to as "in situ biogeochemical transformation" (ISBGT[184]), which includes Biogeochemical Reductive Dechlorination (BiRD)[76,185]—involve stimulation of microbial sulfate reduction to sulfidate indigenous or added iron oxides, thereby producing an in situ reactive treatment zone containing FeS. Since FeS causes dechlorination mainly by β-elimination, it can reduce PCE and TCE with minimal formation of problematic intermediates, under some field conditions.[76,77,185] However, further testing of ISBGT in a more highly controlled field experiment, showed significant accumulation of *cis*-DCE (from TCE), which most likely was due to biotic dechlorination in competition with the desired abiotic process.[174] In both of these scenarios, sulfidogenesis and sulfidation are natural biogeochemical processes, which depend on in situ microbial activity, and are not easily controlled.

In addition to natural sulfidation processes, the recent development of methods for controlled abiotic sulfidation of iron-based materials—the main focus of this review—greatly expands the range of possible applications for contaminant sequestration and degradation in groundwater remediation. Controlled sulfidation allows formation of iron-based materials with more diverse and optimized properties, and may eventually enable materials tailored for use under the conditions of specific sites. The benefits of controlled sulfidation for in situ applications are especially promising for nZVI and mZVI used for emplacement by injection (which is more common than nZVI in current remediation practice). Based on the laboratory work summarized above, sulfidation is expected to decrease reactivity of these materials with H_2O, increase (or not change) their reactivity with contaminants, preserve their selectivity for favorable product formation pathways, and possibly decrease aggregation and thereby increase particle mobility. These expectations are supported by the available data from bench-scale treatability testing—which used nZVI prepared by borohydride reduction and then aqueous-solid sulfidation using dithionite.[86] In that study, 63% of the iron was still Fe(0) after 400 day of aging in anoxic water, and the material still reduced 1,2-DCA at a rate that appeared to be similar to that of freshly sulfidated material. These results suggest sulfidated nZVI may have high efficiency for contaminant reduction, in the short term, and capacity (or longevity) for sustained contaminant degradation in the long term. Furthermore, a field scale pilot-scale study using this sulfidated nZVI is underway, with preliminary data showing the injected material is minimally aggregated (a prerequisite to mobility[186−188]), and at least as mobile as unsulfidated nZVI that was injected in a previous nearby field trial.[189] However, a major uncertainty concerning the ultimate degradation products from sulfidated (n)ZVI applications in the field is the role of microbiological processes. For nonsulfidated nZVI, it has been observed that H_2 generation from ZVI and organic carbon from stabilizers used in many nZVI suspensions during injection (e.g., carboxymethyl cellulose) significantly affect microbial growth and dechlorination long after the initial nZVI is gone.[190] Furthermore, since sulfidated nZVI produces much less H_2 and may persist for significantly longer timeframes, sulfidation may alter the abiotic vs biotic pathways. However, the relative importance of these changes remains to be further investigated.

DOI: 10.1021/acs.est.7b04177
Environ. Sci. Technol. 2017, 51, 13070−13085

It should be emphasized that sulfidation of iron-based materials for environmental applications is an actively evolving area. With the surge of interest in applying iron-based materials for water treatment,[176,181] the implications of sulfidation now extend beyond in situ groundwater remediation to ex situ water treatment (Figure 6, upper-right). However, water treatment differs from groundwater remediation in many respects, including contaminant type and composition, materials applied, engineering control, as well as environmental conditions. Those differences present unique challenges to test the generality and applicability of conclusions and knowledge derived from existing literature that overwhelmingly focuses on groundwater remediation. It is likely that operational variables of sulfidation optimized for groundwater remediation may not suffice for water treatment applications. For example, inhibited corrosion by sulfidation might not be ideal for metals that are better treated by ZVI under enhanced corrosive conditions (e.g., chromate[191,192]). Given the dynamic effects of sulfidation on corrosion (ranging from promoting to inhibitory, as discussed above), such variability might require identifying the niches where sulfidation enhances corrosion. Another example of a new research front is the recent discovery of the formation of reactive oxygen species by reacting O_2 with FeS,[193] which expands the treatment process from reductive to oxidative for sulfidated materials. Whether in situ or ex situ, oxidation reactions can degrade (or sequester) contaminants that are not treatable by reductive processes (e.g., emerging contaminants, such as 1,4-dioxane[194] and per- and polyfluoroalkyl substances (PFASs)[195]). Similarly, additional research will be needed to identify the optimized conditions for treatment in order to demonstrate sulfidated iron-based materials can form the basis for sustainable in situ or ex situ oxidative water treatment/remediation applications. Since redox conditions can be variable under some field conditions (e.g., fluctuating water tables), another possibility is that contaminant removal can involve both the reductive and oxidative processes addressed in this review. The redox chemistry of the multiphase sulfidated iron-based materials under such dynamic conditions will be very complex, but it could eventually form the basis for novel remediation/treatment technologies. In summary, these ongoing and future interests provide new opportunities to fully explore the broader spectrum of the benefits and utility of sulfidation for environmental applications.

■ ASSOCIATED CONTENT

Supporting Information

This material is available free of charge at The Supporting Information is available free of charge on the ACS Publications website at DOI: 10.1021/acs.est.7b04177.

The data used in Figure 4, published XPS spectra, and preliminary TEM characterizations (PDF)

■ AUTHOR INFORMATION

Corresponding Author

*Phone: 503-346-3431; e-mail: tratnyek@ohsu.edu.

ORCID

Paul G. Tratnyek: 0000-0001-8818-6417

Denis M. O'Carroll: 0000-0001-6557-226X

Notes

The authors declare no competing financial interest.

■ ACKNOWLEDGMENTS

This material is based on work supported by the Strategic Environmental Research and Development Program of the U.S. Department of Defense, Award Numbers ER-2308, ER-2620, and ER-2621, the Oak Ridge Institute for Science and Education Fellowship, the Ontario Research Fund—Research Excellence Program (Ontario, Canada) for the ORF-RE-WR01 Project Innovative, Natural Sciences and Engineering Research Council of Canada (NSERC) Engage Program (Grant Number: 449311-14) and Czech Science Foundation (Grant Number GF17-33779L). Salary support was provided by an Australian Research Council Future Fellowship to DMO and an NSERC Industrial Postgraduate Scholarship to ANG. This report has not been subject to review by any sponsor and therefore does not necessarily reflect agency views and no official endorsements should be inferred.

■ REFERENCES

(1) Rickard, D. T. Kinetics and mechanism of the sulfidation of goethite. *Am. J. Sci.* **1974**, *274* (8), 941−952.

(2) Morse, J. W.; Millero, F. J.; Cornwell, J. C.; Rickard, D. The chemistry of the hydrogen sulfide and iron sulfide systems in natural waters. *Earth-Sci. Rev.* **1987**, *24*, 1−42.

(3) Poulton, S. W. Sulfide oxidation and iron dissolution kinetics during the reaction of dissolved sulfide with ferrihydrite. *Chem. Geol.* **2003**, *202* (1), 79−94.

(4) Poulton, S. W.; Krom, M. D.; Raiswell, R. A revised scheme for the reactivity of iron (oxyhydr) oxide minerals towards dissolved sulfide. *Geochim. Cosmochim. Acta* **2004**, *68* (18), 3703−3715.

(5) Slowey, A. J.; Brown, G. E. Transformations of mercury, iron, and sulfur during the reductive dissolution of iron oxyhydroxide by sulfide. *Geochim. Cosmochim. Acta* **2007**, *71* (4), 877−894.

(6) Lee, J.-H.; Zachara, J. M.; Fredrickson, J. K.; Heald, S. M.; McKinley, J. P.; Plymale, A. E.; Resch, C. T.; Moore, D. A. Fe(II)-and sulfide-facilitated reduction of $^{99}Tc(VII)O_4^-$ in microbially reduced hyporheic zone sediments. *Geochim. Cosmochim. Acta* **2014**, *136*, 247−264.

(7) Bennett, D. G.; Gens, R. Overview of European concepts for high-level waste and spent fuel disposal with special reference waste container corrosion. *J. Nucl. Mater.* **2008**, *379* (1), 1−8.

(8) Choudhary, L.; Macdonald, D. D.; Alfantazi, A. Role of thiosulfate in the corrosion of steels: A review. *Corrosion* **2015**, *71* (9), 1147−1168.

(9) Enning, D.; Garrelfs, J. Corrosion of iron by sulfate-reducing bacteria: New views of an old problem. *Appl. Environ. Microbiol.* **2014**, *80* (4), 1226−1236.

(10) Little, B.; Wagner, P. An overview of microbiologically influenced corrosion of metals and alloys used in the storage of nuclear wastes. *Can. J. Microbiol.* **1996**, *42* (4), 367−374.

(11) Little, B. J.; Mansfeld, F. B.; Arps, P. J.; Earthman, J. C. *Microbiologically Influenced Corrosion*; Wiley Online Library, 2007.

(12) Fan, D.; Anitori, R. P.; Tebo, B. M.; Tratnyek, P. G.; Lezama Pacheco, J. S.; Kukkadapu, R. K.; Engelhard, M. H.; Bowden, M. E.; Kovarik, L.; Arey, B. W. Reductive sequestration of pertechnetate ($^{99}TcO_4^-$) by nano zero-valent iron (nZVI) transformed by abiotic sulfide. *Environ. Sci. Technol.* **2013**, *47* (10), 5302−5310.

(13) Fan, D.; O'Brien Johnson, G.; Tratnyek, P. G.; Johnson, R. L. Sulfidation of nano zerovalent iron (nZVI) for improved selectivity during in-situ chemical reduction (ISCR). *Environ. Sci. Technol.* **2016**, *50* (17), 9558−9565.

(14) Kim, E.-J.; Kim, J.-H.; Azad, A.-M.; Chang, Y.-S. Facile synthesis and characterization of Fe/FeS nanoparticles for environmental applications. *ACS Appl. Mater. Interfaces* **2011**, *3* (5), 1457−1462.

(15) Kim, E.-J.; Kim, J.-H.; Chang, Y.-S.; Turcio-Ortega, D.; Tratnyek, P. G. Effects of metal ions on the reactivity and corrosion electrochemistry of Fe/FeS nanoparticles. *Environ. Sci. Technol.* **2014**, *48* (7), 4002−4011.

(16) Kim, E.-J.; Murugesan, K.; Kim, J.-H.; Tratnyek, P. G.; Chang, Y.-S. Remediation of trichloroethylene by FeS-coated iron nanoparticles in simulated and real groundwater: Effects of water chemistry. *Ind. Eng. Chem. Res.* **2013**, *52* (27), 9343−9350.
(17) Rajajayavel, S. R. C.; Ghoshal, S. Enhanced reductive dechlorination of trichloroethylene by sulfidated nanoscale zerovalent iron. *Water Res.* **2015**, *78*, 144−153.
(18) Han, Y.; Yan, W. Reductive Dechlorination of trichloroethene by zero-valent iron nanoparticles: Reactivity enhancement through sulfidation treatment. *Environ. Sci. Technol.* **2016**, *50* (23), 12992−13001.
(19) Su, Y.; Adeleye, A. S.; Huang, Y.; Zhou, X.; Keller, A. A.; Zhang, Y. Direct synthesis of novel and reactive sulfide-modified nano iron through nanoparticle seeding for improved cadmium-contaminated water treatment. *Sci. Rep.* **2016**, *6*, 24358.
(20) Su, Y.; Adeleye, A. S.; Keller, A. A.; Huang, Y.; Dai, C.; Zhou, X.; Zhang, Y. Magnetic sulfide-modified nanoscale zerovalent iron (S-nZVI) for dissolved metal ion removal. *Water Res.* **2015**, *74*, 47−57.
(21) Sun, Q.; Feitz, A. J.; Guan, J.; Waite, T. D. Comparison of the reactivity of nanosized zero-valent iron (nZVI) particles produced by borohydride and dithionite reduction of iron salts. *Nano* **2008**, *3* (5), 341−349.
(22) Du, J.; Bao, J.; Fu, X.; Lu, C.; Kim, S. H. Facile preparation of S/Fe composites as an effective peroxydisulfate activator for RhB degradation. *Sep. Purif. Technol.* **2016**, *163*, 145−152.
(23) Du, J.; Bao, J.; Lu, C.; Werner, D. Reductive sequestration of chromate by hierarchical FeS@Fe^0 particles. *Water Res.* **2016**, *102*, 73−81.
(24) Xu, C.; Zhang, B.; Wang, Y.; Shao, Q.; Zhou, W.; Fan, D.; Bandstra, J. Z.; Shi, Z.; Tratnyek, P. G. Effects of sulfidation, magnetization, and oxygenation on Azo dye reduction by zerovalent iron. *Environ. Sci. Technol.* **2016**, *50* (21), 11879−11887.
(25) Gu, Y.; Wang, B.; He, F.; Bradley, M. J.; Tratnyek, P. G. Mechanochemically sulfidated microscale zero valent iron: Pathways, kinetics, mechanism, and efficiency of trichloroethylene dechlorination. *Environ. Sci. Technol.* **2017**, DOI: 10.1021/acs.est.7b03604.
(26) Du, J.; Bao, J.; Fu, X.; Lu, C.; Kim, S. H. Mesoporous sulfur-modified iron oxide as an effective Fenton-like catalyst for degradation of bisphenol A. *Appl. Catal., B* **2016**, *184*, 132−141.
(27) Scherer, M. M.; Balko, B. A.; Tratnyek, P. G., The role of oxides in reduction reactions at the metal-water interface. In *Mineral-Water Interfacial Reactions*; Donald, L., Sparks, T. J. G., Ed.; ACS Publications, 1998; Vol. *715*, pp. 301−322.
(28) Lipczynska-Kochany, E.; Harms, S.; Milburn, R.; Sprah, G.; Nadarajah, N. Degradation of carbon tetrachloride in the presence of iron and sulphur containing compounds. *Chemosphere* **1994**, *29* (7), 1477−1489.
(29) Hassan, S. M. Reduction of halogenated hydrocarbons in aqueous media: I. Involvement of sulfur in iron catalysis. *Chemosphere* **2000**, *40* (12), 1357−1363.
(30) Benner, S. G.; Blowes, D. W.; Ptacek, C. J.; Mayer, K. U. Rates of sulfate reduction and metal sulfide precipitation in a permeable reactive barrier. *Appl. Geochem.* **2002**, *17* (3), 301−320.
(31) Benner, S. G.; Blowes, D. W.; Gould, W. D.; Herbert, R. B.; Ptacek, C. J. Geochemistry of a permeable reactive barrier for metals and acid mine drainage. *Environ. Sci. Technol.* **1999**, *33* (16), 2793−2799.
(32) Blowes, D. W.; Ptacek, C. J.; Benner, S. G.; McRae, C. W.; Bennett, T. A.; Puls, R. W. Treatment of inorganic contaminants using permeable reactive barriers. *J. Contam. Hydrol.* **2000**, *45* (1), 123−137.
(33) Furukawa, Y.; Kim, J.-W.; Watkins, J.; Wilkin, R. T. Formation of ferrihydrite and associated iron corrosion products in permeable reactive barriers of zero-valent iron. *Environ. Sci. Technol.* **2002**, *36* (24), 5469−5475.
(34) Gu, B.; Phelps, T. J.; Liang, L.; Dickey, M. J.; Roh, Y.; Kinsall, B. L.; Palumbo, A. V.; Jacobs, G. K. Biogeochemical dynamics in zero-valent iron columns: implications for permeable reactive barriers. *Environ. Sci. Technol.* **1999**, *33* (13), 2170−2177.
(35) He, Y. T.; Wilson, J. T.; Wilkin, R. T. Transformation of reactive iron minerals in a permeable reactive barrier (biowall) used to treat TCE in groundwater. *Environ. Sci. Technol.* **2008**, *42* (17), 6690−6696.
(36) Johnson, R. L.; Thoms, R. B.; O'Brien Johnson, R.; Nurmi, J. T.; Tratnyek, P. G. Mineral precipitation upgradient from a zero-valent iron permeable reactive barrier. *Groundwater Monit. Rem.* **2008**, *28* (3), 56−64.
(37) Puls, R. W.; Paul, C. J.; Powell, R. M. The application of in situ permeable reactive (zero-valent iron) barrier technology for the remediation of chromate-contaminated groundwater: A field test. *Appl. Geochem.* **1999**, *14* (81), 989−1000.
(38) Tratnyek, P. G., Permeable reactive barriers of iron and other zero-valent metals. In *Chemical Degradation Methods for Wastes and Pollutants: Environmental and Industrial Applications*; CRC Press, 2003, pp. 371−421.
(39) Wilkin, R. T.; Puls, R. W.; Sewell, G. W. Long-term performance of permeable reactive barriers using zero-valent iron: Geochemical and microbiological effects. *Groundwater* **2003**, *41* (4), 493−503.
(40) Boparai, H. K.; Shea, P. J.; Comfort, S. D.; Snow, D. D. Dechlorinating chloroacetanilide herbicides by dithionite-treated aquifer sediment and surface soil. *Environ. Sci. Technol.* **2006**, *40* (9), 3043−3049.
(41) Istok, J. D.; Amonette, J. E.; Cole, C. R.; Fruchter, J. S.; Humphrey, M. D.; Szecsody, J. E.; Teel, S. S.; Vermeul, V. R.; Williams, M. D.; Yabusaki, S. B. In situ redox manipulation by dithionite injection: Intermediate-scale laboratory experiments. *Groundwater* **1999**, *37* (6), 884−889.
(42) Szecsody, J. E.; Fruchter, J. S.; Williams, M. D.; Vermeul, V. R.; Sklarew, D. In situ chemical reduction of aquifer sediments: Enhancement of reactive iron phases and TCE dechlorination. *Environ. Sci. Technol.* **2004**, *38* (17), 4656−4663.
(43) Hansson, E. B.; Odziemkowski, M. S.; Gillham, R. W. Influence of Na_2S on the degradation kinetics of CCl_4 in the presence of very pure iron. *J. Contam. Hydrol.* **2008**, *98* (3), 128−134.
(44) Hansson, E. B.; Odziemkowski, M. S.; Gillham, R. W. Formation of poorly crystalline iron monosulfides: Surface redox reactions on high purity iron, spectroelectrochemical studies. *Corros. Sci.* **2006**, *48* (11), 3767−3783.
(45) Tratnyek, P. G.; Salter-Blanc, A. J.; Nurmi, J. T.; Amonette, J. E.; Liu, J.; Wang, C.; Dohnalkova, A.; Baer, D. R., Reactivity of zerovalent metals in aquatic media: Effects of organic surface coatings. In *Aquatic Redox Chemistry*; ACS Publications, 2011; Vol. *1071*, pp 381−406.
(46) Barbash, J. E.; Reinhard, M. Abiotic dehalogenation of 1,2-dichloroethane and 1,2-dibromoethane in aqueous solution containing hydrogen sulfide. *Environ. Sci. Technol.* **1989**, *23* (11), 1349−1358.
(47) Roberts, A. L.; Sanborn, P. N.; Gschwend, P. M. Nucleophilic substitution reactions of dihalomethanes with hydrogen sulfide species. *Environ. Sci. Technol.* **1992**, *26* (11), 2263−2274.
(48) Kriegman-King, M. R.; Reinhard, M. Transformation of carbon tetrachloride in the presence of sulfide, biotite, and vermiculite. *Environ. Sci. Technol.* **1992**, *26* (11), 2198−2206.
(49) Kriegman-King, M. R.; Reinhard, M. Transformation of carbon tetrachloride by pyrite in aqueous solution. *Environ. Sci. Technol.* **1994**, *28* (4), 692−700.
(50) Shao, H.; Butler, E. C. Influence of soil minerals on the rates and products of abiotic transformation of carbon tetrachloride in anaerobic soils and sediments. *Environ. Sci. Technol.* **2009**, *43* (6), 1896−1901.
(51) Butler, E. C.; Hayes, K. F. Effects of solution composition and pH on the reductive dechlorination of hexachloroethane by iron sulfide. *Environ. Sci. Technol.* **1998**, *32* (9), 1276−1284.
(52) Butler, E. C.; Hayes, K. F. Kinetics of the transformation of trichloroethylene and tetrachloroethylene by iron sulfide. *Environ. Sci. Technol.* **1999**, *33* (12), 2021−2027.
(53) Butler, E. C.; Hayes, K. F. Kinetics of the transformation of halogenated aliphatic compounds by iron sulfide. *Environ. Sci. Technol.* **2000**, *34* (3), 422−429.
(54) Butler, E. C.; Hayes, K. F. Factors influencing rates and products in the transformation of trichloroethylene by iron sulfide and iron metal. *Environ. Sci. Technol.* **2001**, *35* (19), 3884−3891.

DOI: 10.1021/acs.est.7b04177
Environ. Sci. Technol. 2017, 51, 13070−13085

(55) Choi, J.; Choi, K.; Lee, W. Effects of transition metal and sulfide on the reductive dechlorination of carbon tetrachloride and 1,1,1-trichloroethane by FeS. *J. Hazard. Mater.* **2009**, *162* (2), 1151−1158.
(56) He, Y. T.; Wilson, J. T.; Wilkin, R. T. Impact of iron sulfide transformation on trichloroethylene degradation. *Geochim. Cosmochim. Acta* **2010**, *74* (7), 2025−2039.
(57) Jeong, H. Y.; Hayes, K. F. Reductive dechlorination of tetrachloroethylene and trichloroethylene by mackinawite (FeS) in the presence of metals: Reaction rates. *Environ. Sci. Technol.* **2007**, *41* (18), 6390−6396.
(58) Devlin, J. F.; Müller, D. Field and laboratory studies of carbon tetrachloride transformation in a sandy aquifer under sulfate reducing conditions. *Environ. Sci. Technol.* **1999**, *33* (7), 1021−1027.
(59) Assaf-Anid, N.; Lin, K.-Y. Carbon tetrachloride reduction by Fe^{2+}, S^{2-}, and FeS with vitamin B_{12} as organic amendment. *J. Environ. Eng.* **2002**, *128* (1), 94−99.
(60) Liang, X.; Dong, Y.; Kuder, T.; Krumholz, L. R.; Philp, R. P.; Butler, E. C. Distinguishing abiotic and biotic transformation of tetrachloroethylene and trichloroethylene by stable carbon isotope fractionation. *Environ. Sci. Technol.* **2007**, *41* (20), 7094−7100.
(61) Lan, Y.; Butler, E. C. Iron-sulfide-associated products formed during reductive dechlorination of carbon tetrachloride. *Environ. Sci. Technol.* **2016**, *50* (11), 5489−5497.
(62) Lan, Y.; Madden, A. S. E.; Butler, E. C. Transformation of mackinawite to greigite by trichloroethylene and tetrachloroethylene. *Environ. Sci. Process. Impact.* **2016**, *18* (10), 1266−1273.
(63) Hyun, S. P.; Davis, J. A.; Sun, K.; Hayes, K. F. Uranium(VI) reduction by iron(II) monosulfide mackinawite. *Environ. Sci. Technol.* **2012**, *46* (6), 3369−3376.
(64) Jeong, H. Y.; Klaue, B.; Blum, J. D.; Hayes, K. F. Sorption of mercuric ion by synthetic nanocrystalline mackinawite (FeS). *Environ. Sci. Technol.* **2007**, *41* (22), 7699−7705.
(65) Jeong, H. Y.; Sun, K.; Hayes, K. F. Microscopic and spectroscopic characterization of Hg(II) immobilization by mackinawite (FeS). *Environ. Sci. Technol.* **2010**, *44* (19), 7476−7483.
(66) Mullet, M.; Boursiquot, S.; Ehrhardt, J.-J. Removal of hexavalent chromium from solutions by mackinawite, tetragonal FeS. *Colloids Surf., A* **2004**, *244* (1), 77−85.
(67) Scheinost, A. C.; Charlet, L. Selenite reduction by mackinawite, magnetite and siderite: XAS characterization of nanosized redox products. *Environ. Sci. Technol.* **2008**, *42* (6), 1984−1989.
(68) Wolthers, M.; Charlet, L.; van Der Weijden, C. H.; Van der Linde, P. R.; Rickard, D. Arsenic mobility in the ambient sulfidic environment: Sorption of arsenic (V) and arsenic (III) onto disordered mackinawite. *Geochim. Cosmochim. Acta* **2005**, *69* (14), 3483−3492.
(69) Han, Y.-S.; Jeong, H. Y.; Demond, A. H.; Hayes, K. F. X-ray absorption and photoelectron spectroscopic study of the association of As (III) with nanoparticulate FeS and FeS-coated sand. *Water Res.* **2011**, *45* (17), 5727−5735.
(70) Ding, Q.; Ding, F.; Qian, T.; Zhao, D.; Wang, L. Reductive immobilization of rhenium in soil and groundwater using pyrite nanoparticles. *Water, Air, Soil Pollut.* **2015**, *226* (12), 409.
(71) Gong, Y.; Liu, Y.; Xiong, Z.; Kaback, D.; Zhao, D. Immobilization of mercury in field soil and sediment using carboxymethyl cellulose stabilized iron sulfide nanoparticles. *Nanotechnology* **2012**, *23* (29), 294007.
(72) Gong, Y.; Liu, Y.; Xiong, Z.; Zhao, D. Immobilization of mercury by carboxymethyl cellulose stabilized iron sulfide nanoparticles: reaction mechanisms and effects of stabilizer and water chemistry. *Environ. Sci. Technol.* **2014**, *48* (7), 3986−3994.
(73) Jacob, D. L.; Otte, M. L. Conflicting processes in the wetland plant rhizosphere: Metal retention or mobilization? *Water, Air, Soil Pollut.: Focus* **2003**, *3* (1), 91−104.
(74) Gong, Y.; Tang, J.; Zhao, D. Application of iron sulfide particles for groundwater and soil remediation: A review. *Water Res.* **2016**, *89*, 309−320.
(75) Evans, P. J.; Nguyen, D.; Chappell, R. W.; Whiting, K.; Gillette, J.; Bodour, A.; Wilson, J. T. Factors controlling in situ biogeochemical transformation of trichloroethene: Column study. *Ground Water Monit. R.* **2014**, *34* (3), 65−78.
(76) Kennedy, L. G.; Everett, J. W.; Becvar, E.; DeFeo, D. Field-scale demonstration of induced biogeochemical reductive dechlorination at Dover Air Force Base, Dover, Delaware. *J. Contam. Hydrol.* **2006**, *88* (1), 119−136.
(77) Whiting, K.; Evans, P. J.; Lebrón, C.; Henry, B.; Wilson, J. T.; Becvar, E. Factors controlling in situ biogeochemical transformation of trichloroethene: Field survey. *Ground Water Monit. R.* **2014**, *34* (3), 79−94.
(78) Beaulieu, B.; Ramirez, R. E. Arsenic remediation field study using a sulfate reduction and zero-valent iron PRB. *Ground Water Monit. R.* **2013**, *33* (2), 85−94.
(79) Bruzzoniti, M. C.; Fiore, S. Removal of inorganic contaminants from aqueous solutions: evaluation of the remediation efficiency and of the environmental impact of a zero-valent iron substrate. *Water, Air, Soil Pollut.* **2014**, *225* (9), 2098−2111.
(80) Filip, J.; Slunský, J.; Nosek, J.; Semerád, J.; Kašlík, J.; Oborná, J.; Bachořík, J.; Medřík, I., Sulfidized nZVI particles for groundwater treatment: Synthesis, complex characterization and laboratory-scale testing. *ACS National Meeting, San Francisco, CA* **2017**, Abstract No. 307.
(81) Li, D.; Mao, Z.; Zhong, Y.; Huang, W.; Wu, Y.; Peng, P. a. Reductive transformation of tetrabromobisphenol A by sulfidated nano zerovalent iron. *Water Res.* **2016**, *103*, 1−9.
(82) Li, D.; Zhu, X.; Zhong, Y.; Huang, W.; Peng, P. a. Abiotic transformation of hexabromocyclododecane by sulfidated nanoscale zerovalent iron: Kinetics, mechanism and influencing factors. *Water Res.* **2017**, *121*, 140−149.
(83) Gong, Y.; Gai, L.; Tang, J.; Fu, J.; Wang, Q.; Zeng, E. Y. Reduction of Cr(VI) in simulated groundwater by FeS-coated iron magnetic nanoparticles. *Sci. Total Environ.* **2017**, *595*, 743−751.
(84) Rayaroth, M. P.; Lee, C.-S.; Aravind, U. K.; Aravindakumar, C. T.; Chang, Y.-S. Oxidative degradation of benzoic acid using Fe^0-and sulfidized Fe^0-activated persulfate: A comparative study. *Chem. Eng. J.* **2017**, *315*, 426−436.
(85) Song, S.; Su, Y.; Adeleye, A. S.; Zhang, Y.; Zhou, X. Optimal design and characterization of sulfide-modified nanoscale zerovalent iron for diclofenac removal. *Appl. Catal., B* **2017**, *201*, 211−220.
(86) Nunez Garcia, A.; Boparai, H. K.; O'Carroll, D. M. Enhanced dechlorination of 1,2-dichloroethane by coupled nano iron-dithionite treatment. *Environ. Sci. Technol.* **2016**, *50* (10), 5243−5251.
(87) Xie, Y.; Cwiertny, D. M. Use of dithionite to extend the reactive lifetime of nanoscale zero-valent iron treatment systems. *Environ. Sci. Technol.* **2010**, *44* (22), 8649−8655.
(88) Guo, L.; Chen, F.; Fan, X.; Cai, W.; Zhang, J. S-doped α-Fe_2O_3 as a highly active heterogeneous Fenton-like catalyst towards the degradation of acid orange 7 and phenol. *Appl. Catal., B* **2010**, *96* (1), 162−168.
(89) Tang, J.; Tang, L.; Feng, H.; Zeng, G.; Dong, H.; Zhang, C.; Huang, B.; Deng, Y.; Wang, J.; Zhou, Y. pH-dependent degradation of p-nitrophenol by sulfidated nanoscale zerovalent iron under aerobic or anoxic conditions. *J. Hazard. Mater.* **2016**, *320*, 581−590.
(90) Hellige, K.; Pollok, K.; Larese-Casanova, P.; Behrends, T.; Peiffer, S. Pathways of ferrous iron mineral formation upon sulfidation of lepidocrocite surfaces. *Geochim. Cosmochim. Acta* **2012**, *81*, 69−81.
(91) Zhang, Q.; Guo, W.; Yue, X.; Liu, Z.; Li, X. Degradation of rhodamine B using FeS-coated zero-valent iron nanoparticles in the presence of dissolved oxygen. *Environ. Prog. Sustainable Energy* **2016**, *35* (6), 1673−1678.
(92) Dos Santos Afonso, M.; Stumm, W. Reductive dissolution of iron(III) (hydr)oxides by hydrogen sulfide. *Langmuir* **1992**, *8* (6), 1671−1675.
(93) Lan, Y.; Butler, E. C. Monitoring the transformation of mackinawite to greigite and pyrite on polymer supports. *Appl. Geochem.* **2014**, *50*, 1−6.
(94) Newman, R. C.; Rumash, K.; Webster, B. J. The effect of pre-corrosion on the corrosion rate of steel in neutral solutions containing

DOI: 10.1021/acs.est.7b04177
Environ. Sci. Technol. 2017, 51, 13070−13085

sulphide: Relevance to microbially influenced corrosion. *Corros. Sci.* **1992**, *33* (12), 1877−1884.
(95) Zheng, Y.; Ning, J.; Brown, B.; Young, D.; Nesic, S., Mechanistic study of the effect of iron sulfide layers on hydrogen sulfide corrosion of carbon steel. In *Corrosion*; NACE International: Dallas, TX, 2015; p 5933.
(96) Bai, P.; Liang, Y.; Zheng, S.; Chen, C. Effect of amorphous FeS semiconductor on the corrosion behavior of pipe steel in H_2S-containing environments. *Ind. Eng. Chem. Res.* **2016**, *55* (41), 10932−10940.
(97) El Mendili, Y.; Abdelouas, A.; El Hajj, H.; Bardeau, J. F. Phase transitions of iron sulphides formed by steel microbial corrosion. *RSC Adv.* **2013**, *3* (48), 26343−26351.
(98) Duret-Thual, C.; Costa, D.; Yang, W. P.; Marcus, P. The role of thiosulfates in the pitting corrosion of Fe-17Cr alloys in neutral chloride solution: Electrochemical and XPS study. *Corros. Sci.* **1997**, *39* (5), 913−933.
(99) Turcio-Ortega, D.; Fan, D.; Tratnyek, P. G.; Kim, E.-J.; Chang, Y.-S. Reactivity of Fe/FeS nanoparticles: Electrolyte composition effects on corrosion electrochemistry. *Environ. Sci. Technol.* **2012**, *46* (22), 12484−12492.
(100) Shoesmith, D. W.; Taylor, P.; Bailey, M. G.; Owen, D. G. The formation of ferrous monosulfide polymorphs during the corrosion of iron by aqueous hydrogen sulfide at 21 C. *J. Electrochem. Soc.* **1980**, *127* (5), 1007−1015.
(101) Martin, J. E.; Herzing, A. A.; Yan, W.; Li, X. Q.; Koel, B. E.; Kiely, C. J.; Zhang, W. X. Determination of the oxide layer thickness in core-shell zerovalent iron nanoparticles. *Langmuir* **2008**, *24* (8), 4329−4334.
(102) Liu, A.; Liu, J.; Zhang, W.-X. Transformation and composition evolution of nanoscale zero valent iron (nZVI) synthesized by borohydride reduction in static water. *Chemosphere* **2015**, *119*, 1068−1074.
(103) Yan, W.; Herzing, A. A.; Kiely, C. J.; Zhang, W.-X. Nanoscale zero-valent iron (nZVI): Aspects of the core-shell structure and reactions with inorganic species in water. *J. Contam. Hydrol.* **2010**, *118* (3−4), 96−104.
(104) Sarathy, V.; Tratnyek, P. G.; Nurmi, J. T.; Baer, D. R.; Amonette, J. E.; Chun, C. L.; Penn, R. L.; Reardon, E. J. Aging of iron nanoparticles in aqueous solution: effects on structure and reactivity. *J. Phys. Chem. C* **2008**, *112* (7), 2286−2293.
(105) Fan, D. Reactivity of Reducing Iron Minerals in the Subsurface: Implications for Contaminant Remediation. Part I: Remediation of Technetium by Sulfidated Nano Zerovalent Iron. Ph.D. Thesis, Oregon Health & Science University, 2015.
(106) Levard, C.; Reinsch, B. C.; Michel, F. M.; Oumahi, C.; Lowry, G. V.; Brown, G. E., Jr Sulfidation processes of PVP-coated silver nanoparticles in aqueous solution: impact on dissolution rate. *Environ. Sci. Technol.* **2011**, *45* (12), 5260−5266.
(107) Fan, D.; Anitori, R. P.; Tebo, B. M.; Tratnyek, P. G.; Lezama Pacheco, J. S.; Kukkadapu, R. K.; Kovarik, L.; Engelhard, M. H.; Bowden, M. E. Oxidative remobilization of technetium sequestered by sulfide-transformed nano zerovalent iron. *Environ. Sci. Technol.* **2014**, *48* (13), 7409−7417.
(108) Rosso, K. M.; Vaughan, D. J. Reactivity of sulfide mineral surfaces. *Rev. Mineral. Geochem.* **2006**, *61* (1), 557−607.
(109) Coles, C. A.; Rao, S. R.; Yong, R. N. Lead and cadmium interactions with mackinawite: Retention mechanisms and the role of pH. *Environ. Sci. Technol.* **2000**, *34* (6), 996−1000.
(110) Li, X.-Q.; Zhang, W.-X. Sequestration of metal cations with zerovalent iron nanoparticles a study with high resolution X-ray photoelectron spectroscopy (HR-XPS). *J. Phys. Chem. C* **2007**, *111* (19), 6939−6946.
(111) Li, S.; Wang, W.; Liu, Y.; Zhang, W.-x. Zero-valent iron nanoparticles (nZVI) for the treatment of smelting wastewater: A pilot-scale demonstration. *Chem. Eng. J.* **2014**, *254*, 115−123.
(112) Zhang, Y.; Yan, J.; Dai, C.; Li, Y.; Zhu, Y.; Zhou, X. Sequestration of Ag(I) from aqueous solution as Ag(0) nanostructures by nanoscale zero valent iron (nZVI). *J. Nanopart. Res.* **2015**, *17* (11), 455.
(113) Niazi, N. K.; Burton, E. D. Arsenic sorption to nanoparticulate mackinawite (FeS): An examination of phosphate competition. *Environ. Pollut.* **2016**, *218*, 111−117.
(114) Farquhar, M. L.; Charnock, J. M.; Livens, F. R.; Vaughan, D. J. Mechanisms of arsenic uptake from aqueous solution by interaction with goethite, lepidocrocite, mackinawite, and pyrite: An X-ray absorption spectroscopy study. *Environ. Sci. Technol.* **2002**, *36* (8), 1757−1762.
(115) Hermann, R.; Neumann-Mahlkau, P. The mobility of zinc, cadmium, copper, lead, iron and arsenic in ground water as a function of redox potential and pH. *Sci. Total Environ.* **1985**, *43* (1−2), 1−12.
(116) Kumar, A. R.; Riyazuddin, P. Speciation of selenium in groundwater: Seasonal variations and redox transformations. *J. Hazard. Mater.* **2011**, *192* (1), 263−269.
(117) Wang, Z.; Lee, S.-W.; Kapoor, P.; Tebo, B. M.; Giammar, D. E. Uraninite oxidation and dissolution induced by manganese oxide: A redox reaction between two insoluble minerals. *Geochim. Cosmochim. Acta* **2013**, *100*, 24−40.
(118) Bi, Y.; Hyun, S. P.; Kukkadapu, R. K.; Hayes, K. F. Oxidative dissolution of UO_2 in a simulated groundwater containing synthetic nanocrystalline mackinawite. *Geochim. Cosmochim. Acta* **2013**, *102*, 175−190.
(119) O'Loughlin, E. J.; Boyanov, M. I.; Antonopoulos, D. A.; Kemner, K. M., Redox processes affecting the speciation of technetium, uranium, neptunium, and plutonium in aquatic and terrestrial environments. In *Aquatic Redox Chemistry*; ACS Publications: 2011; Vol. *1071*, pp 477−517.
(120) Wang, Z.; Giammar, D. E., Metal contaminant oxidation mediated by manganese redox cycling in subsurface environment. In *Advances in the Environmental Biogeochemistry of Manganese Oxides*; ACS Publications: 2015; Vol. *1197*, pp 29−50.
(121) Butler, E. C.; Chen, L.; Hansel, C. M.; Krumholz, L. R.; Madden, A. S. E.; Lan, Y. Biological versus mineralogical chromium reduction: Potential for reoxidation by manganese oxide. *Environ. Sci. Process. Impact* **2015**, *17* (11), 1930−1940.
(122) Moon, H. S.; Komlos, J.; Jaffé, P. R. Uranium reoxidation in previously bioreduced sediment by dissolved oxygen and nitrate. *Environ. Sci. Technol.* **2007**, *41* (13), 4587−4592.
(123) McBeth, J. M.; Lear, G.; Lloyd, J. R.; Livens, F. R.; Morris, K.; Burke, I. T. Technetium reduction and reoxidation in aquifer sediments. *Geomicrobiol. J.* **2007**, *24* (3−4), 189−197.
(124) Bi, Y.; Hayes, K. F. Nano-FeS inhibits UO_2 reoxidation under varied oxic conditions. *Environ. Sci. Technol.* **2013**, *48* (1), 632−640.
(125) Jeong, H. Y.; Han, Y.-S.; Park, S. W.; Hayes, K. F. Aerobic oxidation of mackinawite (FeS) and its environmental implication for arsenic mobilization. *Geochim. Cosmochim. Acta* **2010**, *74* (11), 3182−3198.
(126) Fan, D.; O'Carroll, D. M.; Elliott, D. W.; Xiong, Z.; Tratnyek, P. G.; Johnson, R. L.; Nunez Garcia, A. Selectivity of nano zerovalent iron in in situ chemical reduction: Challenges and improvements. *Remediation* **2016**, *26* (4), 27−40.
(127) Cao, Z.; Liu, X.; Xu, J.; Zhang, J.; Yang, Y.; Zhou, J. L.; Xu, X.; Lowry, G. V. Removal of antibiotic florfenicol by sulfide-modified nanoscale zero-walent iron. *Environ. Sci. Technol.* **2017**, *51* (19), 11269−11277.
(128) Pu, M.; Ma, Y.; Wan, J.; Wang, Y.; Huang, M.; Chen, Y. Fe/S doped granular activated carbon as a highly active heterogeneous persulfate catalyst toward the degradation of Orange G and diethyl phthalate. *J. Colloid Interface Sci.* **2014**, *418*, 330−337.
(129) Elsner, M.; Hofstetter, T. B., Current perspectives on the mechanisms of chlorohydrocarbon degradation in subsurface environments: Insight from kinetics, product formation, probe molecules and isotope fractionation. In *Aquatic Redox Chemistry*; Tratnyek, P. G.; Grundl, T. J.; Haderlein, S. B., Eds.; American Chemical Society: Washington, DC, 2011; Vol. *1071*, pp 407−439.
(130) Butler, E. C.; Dong, Y.; Krumholz, L. R.; Liang, X.; Shao, H.; Tan, Y., Rate controlling processes in the transformation of

DOI: 10.1021/acs.est.7b04177
Environ. Sci. Technol. 2017, 51, 13070−13085

tetrachloroethylene and carbon tetrachloride under iron reducing and sulfate reducing conditions. In *Aquatic Redox Chemistry*; Tratnyek, P. G.; Grundl, T. J.; Haderlein, S. B., Eds.; American Chemical Society: Washington, DC, 2011; Vol. *1071*, pp 519−538.

(131) Roberts, A. L.; Totten, L. A.; Arnold, W. A.; Burris, D. R.; Campbell, T. J. Reductive elimination of chlorinated ethylenes by zero-valent metals. *Environ. Sci. Technol.* **1996**, *30* (8), 2654−2659.

(132) Liu, Y.; Majetich, S. A.; Tilton, R. D.; Sholl, D. S.; Lowry, G. V. TCE dechlorination rates, pathways, and efficiency of nanoscale iron particles with different properties. *Environ. Sci. Technol.* **2005**, *39* (5), 1338−1345.

(133) Jeong, H. Y.; Kim, H.; Hayes, K. F. Reductive dechlorination pathways of tetrachloroethylene and trichloroethylene and subsequent transformation of their dechlorination products by mackinawite (FeS) in the presence of metals. *Environ. Sci. Technol.* **2007**, *41* (22), 7736−7743.

(134) Feng, J.; Lim, T.-T. Pathways and kinetics of carbon tetrachloride and chloroform reductions by nano-scale Fe and Fe/Ni particles: Comparison with commercial micro-scale Fe and Zn. *Chemosphere* **2005**, *59* (9), 1267−1277.

(135) Zwank, L.; Elsner, M.; Aeberhard, A.; Schwarzenbach, R. P.; Haderlein, S. B. Carbon isotope fractionation in the reductive dehalogenation of carbon tetrachloride at iron (hydr)oxide and iron sulfide minerals. *Environ. Sci. Technol.* **2005**, *39* (15), 5634−5641.

(136) Farrell, J.; Melitas, N.; Kason, M.; Li, T. Electrochemical and column investigation of iron-mediated reductive dechlorination of trichloroethylene and perchloroethylene. *Environ. Sci. Technol.* **2000**, *34* (12), 2549−2556.

(137) Wang, J.; Farrell, J. Investigating the role of atomic hydrogen on chloroethene reactions with iron using Tafel analysis and electrochemical impedance spectroscopy. *Environ. Sci. Technol.* **2003**, *37* (17), 3891−3896.

(138) Matheson, L. J.; Tratnyek, P. G. Reductive dehalogenation of chlorinated methanes by iron metal. *Environ. Sci. Technol.* **1994**, *28* (12), 2045−2053.

(139) Li, T.; Farrell, J. Reductive dechlorination of trichloroethene and carbon tetrachloride using iron and palladized-iron cathodes. *Environ. Sci. Technol.* **2000**, *34* (1), 173−179.

(140) Liu, Y.; Lowry, G. V. Effect of particle age (Fe^0 Content) and solution pH on nZVI reactivity: H_2 evolution and TCE dechlorination. *Environ. Sci. Technol.* **2006**, *40* (19), 6085−6090.

(141) Gao, L. J.; Conway, B. E. Poisoning effects of arsenic species on H adsorption and kinetic behavior of the H_2 evolution reaction at Pt in KOH solution. *J. Electroanal. Chem.* **1995**, *395* (1−2), 261−71.

(142) Pearce, C. I.; Pattrick, R. A.; Vaughan, D. J. Electrical and magnetic properties of sulfides. *Rev. Mineral. Geochem.* **2006**, *61* (1), 127−180.

(143) Nezamabadi, S. G. Accelerated degradation of chlorinate solvents by nanoscale zero valent iron coated with iron monosulfide and stabilized with carboxymethyl cellulose. M.S. Thesis, Wright State University, 2016.

(144) Johnson, T. L.; Scherer, M. M.; Tratnyek, P. G. Kinetics of halogenated organic compound degradation by iron metal. *Environ. Sci. Technol.* **1996**, *30* (8), 2634−2640.

(145) Balko, B. A.; Tratnyek, P. G. Photo Effects on the Reduction of Carbon Tetrachloride by Zero-Valent Iron. *J. Phys. Chem. B* **1998**, *102* (8), 1459−1465.

(146) Lien, H.-L.; Zhang, W.-X. Transformation of chlorinated methanes by nanoscale iron particles. *J. Environ. Eng.* **1999**, *125* (11), 1042−1047.

(147) Amonette, J. E.; Workman, D. J.; Kennedy, D. W.; Fruchter, J. S.; Gorby, Y. A. Dechlorination of carbon tetrachloride by Fe(II) associated with goethite. *Environ. Sci. Technol.* **2000**, *34* (21), 4606−4613.

(148) Tratnyek, P. G.; Scherer, M. M.; Deng, B.; Hu, S. Effects of natural organic matter, anthropogenic surfactants, and model quinones on the reduction of contaminants by zero-valent iron. *Water Res.* **2001**, *35* (18), 4435−4443.

(149) McCormick, M. L.; Bouwer, E. J.; Adriaens, P. Carbon tetrachloride transformation in a model iron-reducing culture: Relative kinetics of biotic and abiotic reactions. *Environ. Sci. Technol.* **2002**, *36* (3), 403−410.

(150) Danielsen, K. M.; Hayes, K. F. pH dependence of carbon tetrachloride reductive dechlorination by magnetite. *Environ. Sci. Technol.* **2004**, *38* (18), 4745−4752.

(151) Elsner, M.; Haderlein, S. B.; Kellerhals, T.; Luzi, S.; Zwank, L.; Angst, W.; Schwarzenbach, R. P. Mechanisms and products of surface-mediated reductive dehalogenation of carbon tetrachloride by Fe(II) on goethite. *Environ. Sci. Technol.* **2004**, *38* (7), 2058−2066.

(152) Miehr, R.; Tratnyek, P. G.; Bandstra, J. Z.; Scherer, M. M.; Alowitz, M. J.; Bylaska, E. J. The diversity of contaminant reduction reactions by zero-valent iron: Role of the reductate. *Environ. Sci. Technol.* **2004**, *38* (1), 139−147.

(153) Támara, M.; Butler, E. C. Effects of iron purity and groundwater characteristics on rates and products in the degradation of carbon tetrachloride by iron metal. *Environ. Sci. Technol.* **2004**, *38* (6), 1866−1876.

(154) Danielsen, K. M.; Gland, J. L.; Hayes, K. F. Influence of amine buffers on carbon tetrachloride reductive dechlorination by the iron oxide magnetite. *Environ. Sci. Technol.* **2005**, *39* (3), 756−763.

(155) Nurmi, J. T.; Tratnyek, P. G.; Sarathy, V.; Baer, D. R.; Amonette, J. E.; Pecher, K.; Wang, C.; Linehan, J. C.; Matson, D. W.; Penn, R. L.; Driessen, M. D. Characterization and properties of metallic iron nanoparticles: Spectroscopy, electrochemistry, and kinetics. *Environ. Sci. Technol.* **2005**, *39* (5), 1221−1230.

(156) Hanoch, R. J.; Shao, H.; Butler, E. C. Transformation of carbon tetrachloride by bisulfide treated goethite, hematite, magnetite, and kaolinite. *Chemosphere* **2006**, *63*, 323−334.

(157) Song, H.; Carraway, E. R. Reduction of chlorinated methanes by nano-sized zero-valent iron. Kinetics, pathways, and effect of reaction conditions. *Environ. Eng. Sci.* **2006**, *23* (2), 272−284.

(158) Tratnyek, P. G.; Salter, A. J.; Nurmi, J. T.; Sarathy, V., Environmental applications of zerovalent metals: Iron vs. zinc. In *Nanoscale Materials in Chemistry: Environmental Applications*; ACS Publications, 2010; Vol. *1045*, pp 165−178.

(159) Wang, C. B.; Zhang, W. X. Synthesizing nanoscale iron particles for rapid and complete dechlorination of TCE and PCBs. *Environ. Sci. Technol.* **1997**, *31* (7), 2154−2156.

(160) Su, C.; Puls, R. W. Kinetics of trichloroethene reduction by zerovalent iron and tin: Pretreatment effect, apparent activation energy, and intermediate products. *Environ. Sci. Technol.* **1999**, *33* (1), 163−168.

(161) Chen, J. L.; Al-Abed, S. R.; Ryan, J. A.; Li, Z. Effects of pH on dechlorination of trichloroethylene by zero-valent iron. *J. Hazard. Mater.* **2001**, *83* (3), 243−254.

(162) Lee, W.; Batchelor, B. Abiotic reductive dechlorination of chlorinated ethylenes by iron-bearing soil minerals. 1. Pyrite and magnetite. *Environ. Sci. Technol.* **2002**, *36* (23), 5147−5154.

(163) Schrick, B.; Blough, J. L.; Jones, A. D.; Mallouk, T. E. Hydrodechlorination of trichloroethylene to hydrocarbons using bimetallic nickel-iron nanoparticles. *Chem. Mater.* **2002**, *14* (12), 5140−5147.

(164) Ferrey, M. L.; Wilkin, R. T.; Ford, R. G.; Wilson, J. T. Nonbiological removal of cis-dichloroethylene and 1,1-dichloroethylene in aquifer sediment containing magnetite. *Environ. Sci. Technol.* **2004**, *38* (6), 1746−1752.

(165) Tee, Y.-H.; Grulke, E.; Bhattacharyya, D. Role of Ni/Fe nanoparticle composition on the degradation of trichloroethylene from water. *Ind. Eng. Chem. Res.* **2005**, *44* (18), 7062−7070.

(166) Liu, Y.; Phenrat, T.; Lowry, G. V., Effect of groundwater constituents on H_2 evolution and TCE reduction by reactive Fe(0)/Fe-oxide nanoparticles. In *233rd ACS National Meeting*; American Chemical Society, Division of Environmental Chemistry: Chicago, IL, 2007; Vol. *47*, No. 1, pp 397−402.

(167) Shin, M.-C.; Choi, H.-D.; Kim, D.-H.; Baek, K. Effect of surfactant on reductive dechlorination of trichloroethylene by zero-valent iron. *Desalination* **2008**, *223* (1−3), 299−307.

DOI: 10.1021/acs.est.7b04177
Environ. Sci. Technol. 2017, 51, 13070−13085

(168) Phenrat, T.; Liu, Y.; Tilton, R. D.; Lowry, G. V. Adsorbed polyelectrolyte coatings decrease Fe^0 nanoparticle reactivity with TCE in water: Conceptual model and mechanisms. *Environ. Sci. Technol.* **2009**, *43*, 1507−1514.
(169) Wang, W.; Zhou, M. Degradation of trichloroethylene using solvent-responsive polymer coated Fe nanoparticles. *Colloids Surf., A* **2010**, *369*, 232−239.
(170) Velimirovic, M.; Larsson, P.-O.; Simons, Q.; Bastiaens, L. Reactivity screening of microscale zerovalent irons and iron sulfides towards different CAHs under standardized experimental conditions. *J. Hazard. Mater.* **2013**, *252*−*253*, 204−212.
(171) Fan, D.; Chen, S.; Johnson, R. L.; Tratnyek, P. G. Field deployable chemical redox probe for quantitative characterization of carboxymethylcellulose modified nano zerovalent iron. *Environ. Sci. Technol.* **2015**, *49* (17), 10589−10597.
(172) He, F.; Zhao, D.; Paul, C. Field assessment of carboxymethyl cellulose stabilized iron nanoparticles for in situ destruction of chlorinated solvents in source zones. *Water Res.* **2010**, *44* (7), 2360−2370.
(173) Schöftner, P.; Waldner, G.; Lottermoser, W.; Stöger-Pollach, M.; Freitag, P.; Reichenauer, T. G. Electron efficiency of nZVI does not change with variation of environmental parameters. *Sci. Total Environ.* **2015**, *535*, 69−78.
(174) Stroo, H.; Wilson, J.; Evans, P.; Lebron, C.; Henry, B.; Latta, D.; Ghosh, R.; Leeson, A. *In situ Biogeochemical Treatment Demonstration: Lessons Learned from ESTCP Project ER-201124*; SERDP-ESTCP: December, 2015; p 80.
(175) Shi, F.; Zhang, L.; Yang, J.; Lu, M.; Ding, J.; Li, H. Polymorphous FeS corrosion products of pipeline steel under highly sour conditions. *Corros. Sci.* **2016**, *102*, 103−113.
(176) Guan, X.; Sun, Y.; Qin, H.; Li, J.; Lo, I. M.; He, D.; Dong, H. The limitations of applying zero-valent iron technology in contaminants sequestration and the corresponding countermeasures: the development in zero-valent iron technology in the last two decades (1994−2014). *Water Res.* **2015**, *75*, 224−248.
(177) Ma, J.; He, D.; Collins, R. N.; He, C.; Waite, T. D. The tortoise versus the hare-Possible advantages of microparticulate zerovalent iron (mZVI) over nanoparticulate zerovalent iron (nZVI) in aerobic degradation of contaminants. *Water Res.* **2016**, *105*, 331−340.
(178) Mu, Y.; Ai, Z.; Zhang, L. Phosphate shifted oxygen reduction pathway on $Fe@Fe_2O_3$ core−shell nanowires for enhanced reactive oxygen species generation and aerobic 4-chlorophenol degradation. *Environ. Sci. Technol.* **2017**, *51* (14), 8101−8109.
(179) Mylon, S. E.; Sun, Q.; Waite, T. D. Process optimization in use of zero valent iron nanoparticles for oxidative transformations. *Chemosphere* **2010**, *81* (1), 127−131.
(180) Qin, H.; Li, J.; Yang, H.; Pan, B.; Zhang, W.; Guan, X. Coupled effect of ferrous ion and oxygen on the electron selectivity of zerovalent iron for selenate sequestration. *Environ. Sci. Technol.* **2017**, *51* (9), 5090−5097.
(181) Sun, Y.; Li, J.; Huang, T.; Guan, X. The influences of iron characteristics, operating conditions and solution chemistry on contaminants removal by zero-valent iron: A review. *Water Res.* **2016**, *100*, 277−295.
(182) Phillips, D. H.; Gu, B.; Watson, D. B.; Roh, Y.; Liang, L.; Lee, S. Y. Performance evaluation of a zerovalent iron reactive barrier: Mineralogical consequences. *Environ. Sci. Technol.* **2000**, *34* (19), 4169−4176.
(183) Roh, Y.; Lee, S. Y.; Elless, M. P. Characterization of corrosion products in the permeable reactive barriers. *Environ. Geol.* **2000**, *40* (1−2), 184−194.
(184) NAVFAC. *Biogeochemical Transformation Handbook*; Naval Facilities Engineering Command (NAVFAC), October, 2015; p 32.
(185) Kennedy, L. G.; Everett, J. W.; Gonzales, J. Assessment of biogeochemical natural attenuation and treatment of chlorinated solvents, Altus Air Force Base, Altus, Oklahoma. *J. Contam. Hydrol.* **2006**, *83* (3−4), 221−236.
(186) Kocur, C. M.; O'Carroll, D. M.; Sleep, B. E. Impact of nZVI stability on mobility in porous media. *J. Contam. Hydrol.* **2013**, *145*, 17−25.
(187) Johnson, R. L.; Nurmi, J. T.; O'Brien Johnson, G. S.; Fan, D.; O'Brien Johnson, R. L.; Shi, Z.; Salter-Blanc, A. J.; Tratnyek, P. G.; Lowry, G. V. Field-scale transport and transformation of carboxymethylcellulose-stabilized nano zero-valent iron. *Environ. Sci. Technol.* **2013**, *47* (3), 1573−1580.
(188) Shi, Z.; Fan, D.; Johnson, R. L.; Tratnyek, P. G.; Nurmi, J. T.; Wu, Y.; Williams, K. H. Methods for characterizing the fate and effects of nano zerovalent iron during groundwater remediation. *J. Contam. Hydrol.* **2015**, *181*, 17−35.
(189) Kocur, C. M.; Chowdhury, A. I.; Sakulchaicharoen, N.; Boparai, H. K.; Weber, K. P.; Sharma, P.; Krol, M. M.; Austrins, L.; Peace, C.; Sleep, B. E. Characterization of nZVI mobility in a field scale test. *Environ. Sci. Technol.* **2014**, *48* (5), 2862−2869.
(190) Kocur, C. M. D.; Lomheim, L.; Boparai, H. K.; Chowdhury, A. I. A.; Weber, K. P.; Austrins, L. M.; Edwards, E. A.; Sleep, B. E.; O'Carroll, D. M. Contributions of abiotic and biotic dechlorination following carboxymethyl cellulose stabilized nanoscale zero valent iron injection. *Environ. Sci. Technol.* **2015**, *49* (14), 8648−8656.
(191) Feng, P.; Guan, X.; Sun, Y.; Choi, W.; Qin, H.; Wang, J.; Qiao, J.; Li, L. Weak magnetic field accelerates chromate removal by zero-valent iron. *J. Environ. Sci.* **2015**, *31*, 175−183.
(192) Qin, H.; Li, J.; Bao, Q.; Li, L.; Guan, X. Role of dissolved oxygen in metal (loid) removal by zerovalent iron at different pH: its dependence on the removal mechanisms. *RSC Adv.* **2016**, *6* (55), 50144−50152.
(193) Cheng, D.; Yuan, S.; Liao, P.; Zhang, P. Oxidizing impact induced by mackinawite (FeS) nanoparticles at oxic conditions due to production of hydroxyl radicals. *Environ. Sci. Technol.* **2016**, *50* (21), 11646−11653.
(194) Zenker, M. J.; Borden, R. C.; Barlaz, M. A. Occurrence and treatment of 1, 4-dioxane in aqueous environments. *Environ. Eng. Sci.* **2003**, *20* (5), 423−432.
(195) Merino, N.; Qu, Y.; Deeb, R. A.; Hawley, E. L.; Hoffmann, M. R.; Mahendra, S. Degradation and removal methods for perfluoroalkyl and polyfluoroalkyl substances in water. *Environ. Eng. Sci.* **2016**, *33* (9), 615−649.

DOI: 10.1021/acs.est.7b04177
Environ. Sci. Technol. 2017, 51, 13070−13085